

Convolutional Dictionary Learning

Cristina Garcia-Cardona and Brendt Wohlberg

EDICS: IMT-SLM, IMT-LBM, CIF-SBR

Abstract—Convolutional sparse representations are a form of sparse representation with a dictionary that has a structure that is equivalent to convolution with a set of linear filters. While effective algorithms have recently been developed for the convolutional sparse coding problem, the corresponding dictionary learning problem is substantially more challenging. Furthermore, although a number of different approaches have been proposed, the absence of thorough comparisons between them makes it difficult to determine which of them represents the current state of the art. The present work both addresses this deficiency and proposes some new approaches that outperform existing ones in certain contexts. A thorough set of performance comparisons indicates a very wide range of performance differences among the existing and proposed methods, and clearly identifies those that are the most effective.

Index Terms—Sparse Representation, Sparse Coding, Dictionary Learning, Convolutional Sparse Representation

I. INTRODUCTION

Sparse representations [1] have become one of the most widely used and successful models for inverse problems in signal processing, image processing, and computational imaging. The reconstruction of a signal \mathbf{s} from a sparse representation \mathbf{x} with respect to *dictionary* matrix D is linear, i.e. $\mathbf{s} \approx D\mathbf{x}$, but computing the sparse representation given the signal, referred to as *sparse coding*, usually involves solving an optimization problem¹. When solving problems involving images of any significant size, these representations are typically independently applied to sets of overlapping image patches due to the intractability of learning an unstructured dictionary matrix D mapping to a vector space with the dimensionality of the number of pixels in an entire image.

The convolutional form of sparse representations replaces the unstructured dictionary D with a set of linear filters $\{\mathbf{d}_m\}$. In this case the reconstruction of \mathbf{s} from representation $\{\mathbf{x}_m\}$ is $\mathbf{s} \approx \sum_m \mathbf{d}_m * \mathbf{x}_m$, where \mathbf{s} can be an entire image instead of a small image patch. This form of representation was first introduced some time ago under the label *translation-invariant sparse representations* [3], but has recently enjoyed a revival of interest as *convolutional sparse representations*, inspired by *deconvolutional networks* [4] (see [5, Sec. II]). This interest was spurred by the development of more efficient methods for the computationally-expensive *convolutional sparse coding* (CSC) problem [6], [7], [8], [9], and has led to a number of

applications in which the convolutional form provides state-of-the-art performance [10], [11], [12], [13], [14].

The current leading CSC algorithms [8], [9], [15] are all based on the Alternating Direction Method of Multipliers (ADMM) [16], which decomposes the problem into two sub-problems, one of which is solved by soft-thresholding, and the other having a very efficient non-iterative solution in the DFT domain [8]. The design of convolutional dictionary learning (CDL) algorithms is less straightforward. These algorithms adopt the usual approach for standard dictionary learning, alternating between a sparse coding step that updates the sparse representation of the training data given the current dictionary, and a dictionary update step that updates the current dictionary given the new sparse representation. It is the inherent computational cost of the latter update that makes the CDL problem more difficult than the CSC problem.

Most recent batch-mode² CDL algorithms share the structure introduced in [7] (and described in more detail in [20]), the primary features of which are the use of Augmented Lagrangian methods and the solution of the most computationally expensive subproblems in the frequency domain. Earlier algorithms exist (see [5, Sec. II.D] for a thorough literature review), but since they are less effective, we do not consider them here, focusing on subsequent methods:

- [5] Proposed a number of improvements on the algorithm of [7], including more efficient sparse representation and dictionary updates, and a different Augmented Lagrangian structure with better convergence properties (examined in more detail in [21]).
- [22] Proposed a number of dictionary update methods that lead to CDL algorithms with better performance than that of [7].
- [9] Proposed a CDL algorithm that allows the inclusion of a spatial mask in the data fidelity term by exploiting the mask decoupling technique [23].
- [15] Proposed an alternative masked CDL algorithm that has much lower memory requirements than that of [9] and that converges faster in some contexts.

Unfortunately, due to the absence of any thorough performance comparisons between them (for example, [22] provides comparisons with [7] but not [5]), as well as due to the absence of a careful exploration of the optimum choice of algorithm parameters in most of these works, it is quite difficult to determine which of these methods truly represents the state of the art in CDL.

Three other very recent methods are not considered here. The algorithm of [24] addresses a variant of the CDL problem

C. Garcia-Cardona is with CCS Division, Los Alamos, NM 87545, USA
B. Wohlberg is with Theoretical Division, Los Alamos National Laboratory, Los Alamos, NM 87545, USA. Email: brendt@lanl.gov, Tel: +1 505 667 6886, Fax: +1 505 665 5757

This research was supported by the U.S. Department of Energy through the LANL/LDRD Program.

¹We do not consider the analysis form [2] of sparse representations in this work, focusing instead on the more common synthesis.

²We do not consider the very recent online CDL algorithms [17], [18], [19] in this work.

that is customized for neural signal processing and not relevant to most imaging applications, and [25], [26] appeared while we were finalizing this paper, so that it was not feasible to include them in our comparisons.

The main contributions of the present paper are:

- Providing a thorough performance comparison among the different methods proposed in [5], [22], [9], [15], allowing reliable identification of the most effective algorithms.
- Demonstrating that two of the algorithms proposed in [22], with very different derivations, are in fact closely related and fall within the same class of algorithm.
- Proposing a new approach for the CDL problem without a spatial mask that outperforms all existing methods in a serial processing context.
- Proposing new approaches for the CDL problem with a spatial mask that respectively outperform existing methods in serial and parallel processing contexts.
- Carefully examining the sensitivity of the considered CDL algorithms to their parameters, and proposing simple heuristics for parameter selection that provide close to optimal performance.

II. CONVOLUTIONAL DICTIONARY LEARNING

CDL is usually posed in the form of the problem

$$\arg \min_{\{\mathbf{d}_m\}, \{\mathbf{x}_{k,m}\}} \frac{1}{2} \sum_k \left\| \sum_m \mathbf{d}_m * \mathbf{x}_{k,m} - \mathbf{s}_k \right\|_2^2 + \lambda \sum_k \sum_m \|\mathbf{x}_{k,m}\|_1$$

such that $\|\mathbf{d}_m\|_2 = 1 \forall m$, (1)

where the constraint on the norms of filters \mathbf{d}_m is required to avoid the scaling ambiguity between filters and coefficients³. The training images \mathbf{s}_k are considered to be N dimensional vectors, where N is the number of pixels in each image, and we denote the number of filters and the number of training images by M and K respectively. This problem is non-convex in both variables $\{\mathbf{d}_m\}$ and $\{\mathbf{x}_{k,m}\}$, but is convex in $\{\mathbf{x}_{k,m}\}$ with $\{\mathbf{d}_m\}$ constant, and vice versa. As in standard (non-convolutional) dictionary learning, the usual approach to minimizing this functional is to alternate between updates of the sparse representation and the dictionary. The design of a CDL algorithm can therefore be decomposed into three components: the choice of sparse coding algorithm, the choice of dictionary update algorithm, and the choice of coupling mechanism, including how many iterations of each update should be performed before alternating, and which of their internal variables should be transferred across when alternating.

A. Sparse Coding

While a number of greedy matching pursuit type algorithms were developed for translation-invariant sparse representations [5, Sec. II.C], recent algorithms have largely concentrated on a convolutional form of the standard Basis Pursuit DeNoising (BPDN) [27] problem

$$\arg \min_{\mathbf{x}} (1/2) \|D\mathbf{x} - \mathbf{s}\|_2^2 + \lambda \|\mathbf{x}\|_1 . \quad (2)$$

³The constraint $\|\mathbf{d}_m\|_2 \leq 1$ is frequently used instead of $\|\mathbf{d}_m\|_2 = 1$. In practice this does not appear to make a significant difference to the solution.

This form, which we will refer to as Convolutional BPDN (CBPDN), can be written as

$$\arg \min_{\{\mathbf{x}_m\}} \frac{1}{2} \left\| \sum_m \mathbf{d}_m * \mathbf{x}_m - \mathbf{s} \right\|_2^2 + \lambda \sum_m \|\mathbf{x}_m\|_1 . \quad (3)$$

If we define D_m such that $D_m \mathbf{x}_m = \mathbf{d}_m * \mathbf{x}_m$, and

$$D = \begin{pmatrix} D_0 & D_1 & \dots \end{pmatrix} \quad \mathbf{x} = \begin{pmatrix} \mathbf{x}_0 \\ \mathbf{x}_1 \\ \vdots \end{pmatrix} , \quad (4)$$

we can rewrite the CBPDN problem in standard BPDN form Eq. (2). The Multiple Measurement Vector (MMV) version of CBPDN, for multiple images, can be written as

$$\arg \min_{\{\mathbf{x}_{k,m}\}} \frac{1}{2} \sum_k \left\| \sum_m \mathbf{d}_m * \mathbf{x}_{k,m} - \mathbf{s}_k \right\|_2^2 + \lambda \sum_k \sum_m \|\mathbf{x}_{k,m}\|_1 , \quad (5)$$

where \mathbf{s}_k is the k^{th} image, and $\mathbf{x}_{k,m}$ is the coefficient map corresponding to the k^{th} image and m^{th} dictionary filter. By defining

$$\mathbf{x}_k = \begin{pmatrix} \mathbf{x}_{k,0} \\ \mathbf{x}_{k,1} \\ \vdots \end{pmatrix} \quad X = \begin{pmatrix} \mathbf{x}_0 & \mathbf{x}_1 & \dots \end{pmatrix} \\ S = \begin{pmatrix} \mathbf{s}_0 & \mathbf{s}_1 & \dots \end{pmatrix} , \quad (6)$$

we can rewrite in the MMV form of standard BPDN,

$$\arg \min_X (1/2) \|DX - S\|_F^2 + \lambda \|X\|_1 . \quad (7)$$

The most effective solution for solving Eq. (5) is currently based on ADMM [16]⁴, which solves problems of the form

$$\arg \min_{\mathbf{x}, \mathbf{y}} f(\mathbf{x}) + g(\mathbf{y}) \quad \text{such that} \quad A\mathbf{x} + B\mathbf{y} = \mathbf{c} \quad (8)$$

by iterating over the steps

$$\mathbf{x}^{(j+1)} = \arg \min_{\mathbf{x}} f(\mathbf{x}) + \frac{\rho}{2} \left\| A\mathbf{x} + B\mathbf{y}^{(j)} - \mathbf{c} + \mathbf{u}^{(j)} \right\|_2^2 \quad (9)$$

$$\mathbf{y}^{(j+1)} = \arg \min_{\mathbf{y}} g(\mathbf{y}) + \frac{\rho}{2} \left\| A\mathbf{x}^{(j+1)} + B\mathbf{y} - \mathbf{c} + \mathbf{u}^{(j)} \right\|_2^2 \quad (10)$$

$$\mathbf{u}^{(j+1)} = \mathbf{u}^{(j)} + A\mathbf{x}^{(j+1)} + B\mathbf{y}^{(j+1)} - \mathbf{c} , \quad (11)$$

where *penalty parameter* ρ is an algorithm parameter that plays an important role in determining the convergence rate of the iterations, and \mathbf{u} is the *dual variable* corresponding to the constraint $A\mathbf{x} + B\mathbf{y} = \mathbf{c}$. We can apply ADMM to problem Eq. (7) (working with this form of the problem instead of Eq. (5) simplifies the notation, but the reader should keep in mind that D , X , and S denote the specific block-structured matrices defined above) by *variable splitting*, introducing an auxiliary variable Y that is constrained to be equal to the primary variable X , leading to the equivalent problem

$$\arg \min_{X, Y} (1/2) \|DX - S\|_F^2 + \lambda \|Y\|_1 \quad \text{s.t.} \quad X = Y , \quad (12)$$

⁴It is worth noting, however, that a solution based on FISTA with the gradient computed in the frequency domain, while generally less effective than the ADMM solution, exhibits a relatively small performance difference for the larger λ values typically used for CDL [5, Sec. IV.B].

for which we have the ADMM iterations

$$X^{(j+1)} = \arg \min_X \frac{1}{2} \|DX - S\|_F^2 + \frac{\rho}{2} \|X - Y^{(j)} + U^{(j)}\|_F^2 \quad (13)$$

$$Y^{(j+1)} = \arg \min_Y \lambda \|Y\|_1 + \frac{\rho}{2} \|X^{(j+1)} - Y + U^{(j)}\|_F^2 \quad (14)$$

$$U^{(j+1)} = U^{(j)} + X^{(j+1)} - Y^{(j+1)}. \quad (15)$$

Step Eq. (15) involves simple arithmetic, and step Eq. (14) has a closed-form solution

$$Y^{(j+1)} = \mathcal{S}_{\lambda/\rho} \left(X^{(j+1)} + U^{(j)} \right), \quad (16)$$

where $\mathcal{S}_\gamma(\cdot)$ is the soft-thresholding function

$$\mathcal{S}_\gamma(V) = \text{sign}(V) \odot \max(0, |V| - \gamma), \quad (17)$$

with $\text{sign}(\cdot)$ and $|\cdot|$ of a vector considered to be applied element-wise, and \odot denoting element-wise multiplication. The most computationally expensive step is Eq. (13), which requires solving the linear system

$$(D^T D + \rho I)X = D^T X + \rho(Y - U). \quad (18)$$

Since $D^T D$ is a very large matrix, it is impractical to solve this linear system using the approaches that are effective when D is not a convolutional dictionary. It is possible, however, to exploit the FFT for efficient implementation of the convolution via the DFT convolution theorem. Transforming Eq. (18) into the DFT domain gives

$$(\hat{D}^H \hat{D} + \rho I)\hat{X} = \hat{D}^H \hat{X} + \rho(\hat{Y} - \hat{U}), \quad (19)$$

where \hat{Z} denotes the DFT of variable Z . Due to the structure of \hat{D} , which consists of concatenated diagonal matrices \hat{D}_m , linear system Eq. (19) can be decomposed into a set of N independent linear systems [7], each of which has a left hand side consisting of a diagonal matrix plus a rank-one component, which can be solved very efficiently by exploiting the Sherman-Morrison formula [8].

B. Dictionary Update

The dictionary update requires solving the problem

$$\arg \min_{\{\mathbf{d}_m\}} \frac{1}{2} \sum_k \left\| \sum_m \mathbf{x}_{k,m} * \mathbf{d}_m - \mathbf{s}_k \right\|_2^2 \text{ s.t. } \|\mathbf{d}_m\|_2 = 1, \quad (20)$$

which is a convolutional form of Method of Optimal Directions (MOD) [28] with a constraint on the filter normalization. As for CSC, we will develop the algorithms for solving this problem in the spatial domain, but will solve the critical sub-problems in the frequency domain. We want solve for $\{\mathbf{d}_m\}$ with a relatively small support, but when computing convolutions in the frequency domain we need to work with \mathbf{d}_m that have been zero-padded to the common spatial dimensions of $\mathbf{x}_{k,m}$ and \mathbf{s}_k . The most straightforward way of dealing with this complication is to consider the \mathbf{d}_m to be zero-padded and add a constraint that requires that they be zero outside of the desired support. If we denote the projection operator that zeros the regions of the filters outside of the desired support by P , we can write a constraint set that combines this support constraint with the normalization constraint as

$$C_{\text{PN}} = \{\mathbf{x} \in \mathbb{R}^N : (I - P)\mathbf{x} = 0, \|\mathbf{x}\|_2 = 1\}, \quad (21)$$

and write the dictionary update as

$$\arg \min_{\{\mathbf{d}_m\}} \frac{1}{2} \sum_k \left\| \sum_m \mathbf{x}_{k,m} * \mathbf{d}_m - \mathbf{s}_k \right\|_2^2 \text{ s.t. } \mathbf{d}_m \in C_{\text{PN}} \forall m. \quad (22)$$

Introducing the indicator function $\iota_{C_{\text{PN}}}$ of the constraint set C_{PN} , where the indicator function of a set S is defined as

$$\iota_S(X) = \begin{cases} 0 & \text{if } X \in S \\ \infty & \text{if } X \notin S \end{cases}, \quad (23)$$

allows Eq. (22) to be written in unconstrained form [29]

$$\arg \min_{\{\mathbf{d}_m\}} \frac{1}{2} \sum_k \left\| \sum_m \mathbf{x}_{k,m} * \mathbf{d}_m - \mathbf{s}_k \right\|_2^2 + \sum_m \iota_{C_{\text{PN}}}(\mathbf{d}_m). \quad (24)$$

Defining $X_{k,m}$ such that $X_{k,m} \mathbf{d}_m = \mathbf{x}_{k,m} * \mathbf{d}_m$ and

$$X_k = (X_{k,0} \ X_{k,1} \ \dots) \quad \mathbf{d} = \begin{pmatrix} \mathbf{d}_0 \\ \mathbf{d}_1 \\ \vdots \end{pmatrix} \quad (25)$$

this problem can be expressed as

$$\arg \min_{\mathbf{d}} \frac{1}{2} \sum_k \left\| X_k \mathbf{d} - \mathbf{s}_k \right\|_2^2 + \iota_{C_{\text{PN}}}(\mathbf{d}), \quad (26)$$

or, defining

$$X = \begin{pmatrix} X_{0,0} & X_{0,1} & \dots \\ X_{1,0} & X_{1,1} & \dots \\ \vdots & \vdots & \ddots \end{pmatrix} \quad \mathbf{s} = \begin{pmatrix} \mathbf{s}_0 \\ \mathbf{s}_1 \\ \vdots \end{pmatrix}, \quad (27)$$

as

$$\arg \min_{\mathbf{d}} \frac{1}{2} \left\| X \mathbf{d} - \mathbf{s} \right\|_2^2 + \iota_{C_{\text{PN}}}(\mathbf{d}). \quad (28)$$

Algorithms for solving this problem will be discussed in Sec. III. A common feature of most of these methods is the need to solve a linear system that includes the data fidelity term $(1/2) \|X \mathbf{d} - \mathbf{s}\|_2^2$. As in the case of the X step Eq. (13) for CSC, this problem can be solved in the frequency domain, but there is a critical difference: $\hat{X}^H \hat{X}$ is composed of independent components of rank K instead of rank 1, so that the very efficient Sherman Morrison solution cannot be directly exploited. It is this property that makes the dictionary update inherently more computationally expensive than the sparse coding stage, complicating the design of algorithms, and leading to the present situation in which there is far less clarity as to the best choice of dictionary learning algorithm than there is for the choice of the sparse coding algorithm.

C. Update Coupling

Both sparse coding and dictionary update stages are typically solved via iterative algorithms, and many of these algorithms have more than one working variable that can be used to represent the current solution. The major design choices in coupling the alternating optimization of these two stages are therefore:

- 1) how many iterations of each subproblem to perform before switching to the other subproblem, and

2) which working variable from each subproblem to pass across to the other subproblem.

Since these issues are addressed in detail in [21], we only summarize the conclusions here:

- When both subproblems are solved by ADMM algorithms, most authors have coupled the subproblems via the primary variables (corresponding, for example, to X in Eq. (12)) of each ADMM algorithm.
- This choice tends to be rather unstable, and requires either multiple iterations of each subproblem before alternating, or very large penalty parameters, which can lead to slow convergence.
- The alternative strategy of coupling the subproblems via the auxiliary variables (corresponding, for example, to Y in Eq. (12)) of each ADMM algorithm tends to be more stable, not requiring multiple iterations before alternating, and converging faster.

III. DICTIONARY UPDATE ALGORITHMS

Since the choice of the best CSC algorithm is not in serious dispute, the focus of this work is on the choice of dictionary update algorithm.

A. ADMM with Equality Constraint

The simplest approach to solving Eq. (28) via an ADMM algorithm is to apply the variable splitting

$$\arg \min_{\mathbf{d}, \mathbf{g}} \frac{1}{2} \|X\mathbf{d} - \mathbf{s}\|_2^2 + \iota_{C_{\text{PN}}}(\mathbf{g}) \quad \text{s.t.} \quad \mathbf{d} = \mathbf{g}, \quad (29)$$

for which the corresponding ADMM iterations are

$$\mathbf{d}^{(j+1)} = \arg \min_{\mathbf{d}} \frac{1}{2} \|X\mathbf{d} - \mathbf{s}\|_2^2 + \frac{\sigma}{2} \|\mathbf{d} - \mathbf{g}^{(j)} + \mathbf{h}^{(j)}\|_2^2 \quad (30)$$

$$\mathbf{g}^{(j+1)} = \arg \min_{\mathbf{g}} \iota_{C_{\text{PN}}}(\mathbf{g}) + \frac{\sigma}{2} \|\mathbf{d}^{(j+1)} - \mathbf{g} + \mathbf{h}^{(j)}\|_2^2 \quad (31)$$

$$\mathbf{h}^{(j+1)} = \mathbf{h}^{(j)} + \mathbf{d}^{(j+1)} - \mathbf{g}^{(j+1)}. \quad (32)$$

Step Eq. (31) is of the form

$$\arg \min_{\mathbf{x}} \frac{1}{2} \|\mathbf{x} - \mathbf{y}\|_2^2 + \iota_{C_{\text{PN}}}(\mathbf{x}) = \text{prox}_{\iota_{C_{\text{PN}}}}(\mathbf{y}). \quad (33)$$

It is clear from the geometry of the problem that

$$\text{prox}_{\iota_{C_{\text{PN}}}}(\mathbf{y}) = \frac{PP^T \mathbf{y}}{\|PP^T \mathbf{y}\|_2}, \quad (34)$$

or, if the normalisation $\|\mathbf{d}_m\|_2 \leq 1$ is desired instead,

$$\text{prox}_{\iota_{C_{\text{PN}}}}(\mathbf{y}) = \begin{cases} PP^T \mathbf{y} & \text{if } \|PP^T \mathbf{y}\|_2 \leq 1 \\ \frac{PP^T \mathbf{y}}{\|PP^T \mathbf{y}\|_2} & \text{if } \|PP^T \mathbf{y}\|_2 > 1 \end{cases}. \quad (35)$$

Step Eq. (30) involves solving the linear system

$$(X^T X + \sigma I)\mathbf{d} = X^T \mathbf{s} + \sigma(\mathbf{g} - \mathbf{h}), \quad (36)$$

which can be expressed in the DFT domain as

$$(\hat{X}^H \hat{X} + \sigma I)\hat{\mathbf{d}} = \hat{X}^H \hat{\mathbf{s}} + \sigma(\hat{\mathbf{g}} - \hat{\mathbf{h}}). \quad (37)$$

As in Eq. (19), this linear system can be decomposed into a set of N independent linear systems, but in contrast to Eq. (19), each of these has a left hand side consisting of a diagonal

matrix plus a rank K component, which precludes direct use of the Sherman-Morrison formula [5].

We consider three different approaches to solving these linear systems:

1) *Conjugate Gradient*: An obvious approach to solving Eq. (37) without having to explicitly construct the matrix $\hat{X}^H \hat{X} + \sigma I$ is to apply an iterative method such as Conjugate Gradient (CG). The experiments reported in [5] indicated that solving this system to a relative residual tolerance of 10^{-3} or better is sufficient for the dictionary learning algorithm to converge reliably. The number of CG iterations required can be substantially reduced by using the solution from the previous outer iteration as an initial value.

2) *Iterated Sherman-Morrison*: Since the independent linear systems into which Eq. (37) can be decomposed have left hand side consisting of a diagonal matrix plus a rank K component, one can iteratively apply the Sherman-Morrison formula to obtain a solution [5]. This approach is very effective for small to moderate K , but performs poorly for large K since the computational cost is $\mathcal{O}(K^2)$.

3) *Spatial Tiling*: When $K = 1$, Eq. (37) the very efficient solution via the Sherman-Morrison formula is possible. As pointed out in [22], larger set of training images can be spatially tiled to form a single large image, so that the problem is solved with $K' = 1$.

B. Consensus Framework

In this section it is convenient to introduce different block-matrix and vector notation for the coefficient maps and dictionary, but we overload the usual symbols to emphasize their corresponding roles. We define X_k as in Eq. (25), but define

$$X = \begin{pmatrix} X_0 & 0 & \dots \\ 0 & X_1 & \dots \\ \vdots & \vdots & \ddots \end{pmatrix} \quad \mathbf{d}_k = \begin{pmatrix} \mathbf{d}_{k,0} \\ \mathbf{d}_{k,1} \\ \vdots \end{pmatrix} \quad \mathbf{d} = \begin{pmatrix} \mathbf{d}_0 \\ \mathbf{d}_1 \\ \vdots \end{pmatrix} \quad (38)$$

where $\mathbf{d}_{k,m}$ is distinct copy of dictionary filter m corresponding to training image k .

As proposed in [22], we can pose problem Eq. (28) in the form of an ADMM Consensus problem [16, Ch. 7]

$$\arg \min_{\mathbf{d}} \frac{1}{2} \|X\mathbf{d} - \mathbf{s}\|_2^2 + \iota_{C_{\text{PN}}}(\mathbf{g}) \quad \text{s.t.} \quad \mathbf{g} = \mathbf{d}_k \quad \forall k. \quad (39)$$

The constraint can be written in standard ADMM form as

$$\mathbf{d} - E\mathbf{g} = 0, \quad (40)$$

where

$$E = (I \ I \ \dots)^T. \quad (41)$$

The corresponding ADMM iterations are

$$\mathbf{d}^{(j+1)} = \arg \min_{\mathbf{d}} \frac{1}{2} \|X\mathbf{d} - \mathbf{s}\|_2^2 + \frac{\sigma}{2} \|\mathbf{d} - E\mathbf{g}^{(j)} + \mathbf{h}^{(j)}\|_2^2 \quad (42)$$

$$\mathbf{g}^{(j+1)} = \arg \min_{\mathbf{g}} \iota_{C_{\text{PN}}}(\mathbf{g}) + \frac{\sigma}{2} \|\mathbf{d}^{(j+1)} - E\mathbf{g} + \mathbf{h}^{(j)}\|_2^2 \quad (43)$$

$$\mathbf{h}^{(j+1)} = \mathbf{h}^{(j)} + E\mathbf{d}^{(j+1)} - \mathbf{g}^{(j+1)}. \quad (44)$$

Since X is block diagonal, Eq. (42) can be solved as the K independent problems

$$\mathbf{d}_k^{(j+1)} = \arg \min_{\mathbf{d}_k} \frac{1}{2} \|X_k \mathbf{d}_k - \mathbf{s}_k\|_2^2 + \frac{\sigma}{2} \|\mathbf{d}_k - \mathbf{g}^{(j)} + \mathbf{h}^{(j)}\|_2^2, \quad (45)$$

each of which can be solved via the same efficient DFT-domain Sherman-Morrison method used for Eq. (13). Sub-problem Eq. (43) can be expressed as [16, Sec. 7.1.1]

$$\mathbf{g}^{(j+1)} = \arg \min_{\mathbf{g}} \iota_{C_{\text{PN}}}(\mathbf{g}) + \quad (46)$$

$$\frac{K\sigma}{2} \left\| \mathbf{g} - K^{-1} \left(\sum_{k=0}^{K-1} \mathbf{d}_k^{(j+1)} + \sum_{k=0}^{K-1} \mathbf{h}_k^{(j)} \right) \right\|_2^2 \quad (47)$$

which has the closed-form solution

$$\mathbf{g}^{(j+1)} = \text{prox}_{\iota_{C_{\text{PN}}}} \left(K^{-1} \left(\sum_{k=0}^{K-1} \mathbf{d}_k^{(j+1)} + \sum_{k=0}^{K-1} \mathbf{h}_k^{(j)} \right) \right). \quad (48)$$

C. 3D / Frequency Domain Consensus

Like spatial tiling (see Sec. III-A3), the ‘‘3D’’ method proposed in [22] maps the dictionary update problem with $K > 1$ to an equivalent problem for which $K' = 1$. The ‘‘3D’’ method achieves this by considering an array of K 2D training images as a single 3D training volume. The corresponding dictionary filters are also inherently 3D, but the constraint is modified to require that they are zero other than in the first 3D slice (this can be viewed as an extension of the constraint that the spatially-padded filters are zero except on their desired support) so that the final results is a set of 2D filters, as desired.

While ADMM consensus and ‘‘3D’’ were proposed as two entirely distinct methods [22], it turns out they are closely related: the ‘‘3D’’ method is ADMM consensus with the data fidelity term and constraint expressed in the DFT domain. Since the notation is a bit cumbersome, the point will be illustrated for the $K = 2$ case, but the argument is easily generalised to arbitrary K .

When $K = 2$, the dictionary update problem can be expressed as

$$\arg \min_{\mathbf{d}} \frac{1}{2} \left\| \begin{pmatrix} X_0 \\ X_1 \end{pmatrix} \mathbf{d} - \begin{pmatrix} \mathbf{s}_0 \\ \mathbf{s}_1 \end{pmatrix} \right\|_2^2 + \iota_{C_{\text{PN}}}(\mathbf{d}), \quad (49)$$

which can be rewritten as the equivalent problem⁵

$$\arg \min_{\mathbf{d}_0, \mathbf{d}_1} \frac{1}{2} \left\| \begin{pmatrix} X_0 & X_1 \\ X_1 & X_0 \end{pmatrix} \begin{pmatrix} \mathbf{d}_0 \\ \mathbf{d}_1 \end{pmatrix} - \begin{pmatrix} \mathbf{s}_0 \\ \mathbf{s}_1 \end{pmatrix} \right\|_2^2 + \iota_{C_{\text{PN}}}(\mathbf{g})$$

$$\text{s.t. } \mathbf{d}_0 = \mathbf{g} \quad \mathbf{d}_1 = \mathbf{0}, \quad (50)$$

where the constraint can also be written as

$$\begin{pmatrix} \mathbf{d}_0 \\ \mathbf{d}_1 \end{pmatrix} = \begin{pmatrix} I \\ 0 \end{pmatrix} \mathbf{g}. \quad (51)$$

The general form of the matrix in Eq. (50) is a block-circulant matrix constructed from the blocks X_k . Since the multiplication of the dictionary block vector by the block-circulant matrix is equivalent to convolution in an additional dimension, this equivalent problem represents the ‘‘3D’’ method.

Now, define the un-normalised 2×2 block DFT matrix operating in this extra dimension as

$$F = \begin{pmatrix} I & I \\ I & -I \end{pmatrix}, \quad (52)$$

⁵Equivalence when the constraints are satisfied is easily verified by multiplying out the matrix-vector product in the data fidelity term in Eq. (50).

and apply it to the objective function and constraint, giving

$$\arg \min_{\mathbf{d}_0, \mathbf{d}_1} \frac{1}{2} \left\| F \begin{pmatrix} X_0 & X_1 \\ X_1 & X_0 \end{pmatrix} F^{-1} F \begin{pmatrix} \mathbf{d}_0 \\ \mathbf{d}_1 \end{pmatrix} - F \begin{pmatrix} \mathbf{s}_0 \\ \mathbf{s}_1 \end{pmatrix} \right\|_2^2$$

$$+ \iota_{C_{\text{PN}}}(\mathbf{g}) \quad \text{s.t.} \quad F \begin{pmatrix} \mathbf{d}_0 \\ \mathbf{d}_1 \end{pmatrix} = F \begin{pmatrix} I \\ 0 \end{pmatrix} \mathbf{g}. \quad (53)$$

Since the DFT diagonalises a circulant matrix, this is

$$\arg \min_{\mathbf{d}_0, \mathbf{d}_1} \frac{1}{2} \left\| \begin{pmatrix} X_0 + X_1 & 0 \\ 0 & X_0 - X_1 \end{pmatrix} \begin{pmatrix} \mathbf{d}_0 + \mathbf{d}_1 \\ \mathbf{d}_0 - \mathbf{d}_1 \end{pmatrix} - \begin{pmatrix} \mathbf{s}_0 + \mathbf{s}_1 \\ \mathbf{s}_0 - \mathbf{s}_1 \end{pmatrix} \right\|_2^2$$

$$+ \iota_{C_{\text{PN}}}(\mathbf{g}) \quad \text{s.t.} \quad \begin{pmatrix} \mathbf{d}_0 + \mathbf{d}_1 \\ \mathbf{d}_0 - \mathbf{d}_1 \end{pmatrix} = \begin{pmatrix} \mathbf{g} \\ \mathbf{g} \end{pmatrix}. \quad (54)$$

In this form the problem is an ADMM consensus problem in variables

$$X'_0 = X_0 + X_1 \quad \mathbf{d}'_0 = \mathbf{d}_0 + \mathbf{d}_1 \quad \mathbf{s}'_0 = \mathbf{s}_0 + \mathbf{s}_1$$

$$X'_1 = X_0 - X_1 \quad \mathbf{d}'_1 = \mathbf{d}_0 - \mathbf{d}_1 \quad \mathbf{s}'_1 = \mathbf{s}_0 - \mathbf{s}_1. \quad (55)$$

D. FISTA

The Fast Iterative Shrinkage-Thresholding Algorithm (FISTA) [30], an accelerated proximal gradient method, has been used for CSC [6], [5], [18], and in a recent online CDL algorithm [17], but has not previously been considered for the dictionary update of a batch-mode dictionary learning algorithm.

The FISTA iterations for solving Eq. (28) are

$$\mathbf{y}^{(j+1)} = \text{prox}_{\iota_{C_{\text{PN}}}} \left(\mathbf{d}^{(j)} - \frac{1}{L} \nabla_{\mathbf{d}} \left(\frac{1}{2} \|X\mathbf{d} - \mathbf{s}\|_2^2 \right) \right) \quad (56)$$

$$t^{(j+1)} = \frac{1}{2} \left(1 + \sqrt{1 + 4(t^{(j)})^2} \right) \quad (57)$$

$$\mathbf{d}^{(j+1)} = \mathbf{y}^{(j+1)} + \frac{t^{(j)} - 1}{t^{(j+1)}} \left(\mathbf{y}^{(j+1)} - \mathbf{d}^{(j)} \right), \quad (58)$$

where $t^0 = 1$ and $L > 0$ is a parameter controlling the gradient descent step size. Parameter L can be computed adaptively by using a backtracking step size rule [30], but in the experiments reported here we use a constant L for simplicity. We compute the gradient of the data fidelity term $(1/2) \|X\mathbf{d} - \mathbf{s}\|_2^2$ in Eq. (56) in the DFT domain

$$\nabla_{\mathbf{d}} \left(\frac{1}{2} \|\hat{X}\hat{\mathbf{d}} - \hat{\mathbf{s}}\|_2^2 \right) = \hat{X}^H (\hat{X}\hat{\mathbf{d}} - \hat{\mathbf{s}}), \quad (59)$$

as advocated in [5] for the FISTA solution of the CSC problem.

IV. MASKED CONVOLUTIONAL DICTIONARY LEARNING

When we wish to learn a dictionary from data with missing samples, or have reason to be concerned about the possibility of boundary artifacts resulting from the circular boundary conditions associated with the computation of the convolutions in the DFT domain, it is useful to introduce a variant of Eq. (1) that includes a spatial mask [9], which can be represented by a diagonal matrix W

$$\arg \min_{\{\mathbf{d}_m\}, \{\mathbf{x}_{k,m}\}} \frac{1}{2} \sum_k \left\| W \left(\sum_m \mathbf{d}_m * \mathbf{x}_{k,m} - \mathbf{s}_k \right) \right\|_2^2 +$$

$$\lambda \sum_k \sum_m \|\mathbf{x}_{k,m}\|_1 \quad \text{s.t.} \quad \|\mathbf{d}_m\|_2 = 1 \quad \forall m. \quad (60)$$

As in Sec. II, we separately consider the sparse coding and dictionary updates components of this functional.

A. Sparse Coding

A masked form of the MMV CBPDN problem Eq. (7) can be expressed as the problem⁶

$$\arg \min_X \frac{1}{2} \left\| W(DX - S) \right\|_F^2 + \lambda \|S\|_1. \quad (61)$$

There are two different methods for solving this problem. The one, proposed in [9], exploits the mask decoupling technique [23], involving applying an alternative variable splitting to give the ADMM problem

$$\begin{aligned} \arg \min_X \frac{1}{2} \|WY_1\|_F^2 + \lambda \|Y_0\|_1 \\ \text{s.t. } Y_0 = X \quad Y_1 = DX - S, \end{aligned} \quad (62)$$

where the constraint can also be written as

$$\begin{pmatrix} Y_0 \\ Y_1 \end{pmatrix} = \begin{pmatrix} I \\ D \end{pmatrix} X - \begin{pmatrix} 0 \\ S \end{pmatrix}. \quad (63)$$

The corresponding ADMM iterations are

$$\begin{aligned} X^{(j+1)} = \arg \min_X \frac{\rho}{2} \left\| DX - (Y_1^{(j)} + S - U_1^{(j)}) \right\|_F^2 + \\ \frac{\rho}{2} \left\| X - (Y_0^{(j)} - U_0^{(j)}) \right\|_F^2 \end{aligned} \quad (64)$$

$$Y_0^{(j+1)} = \arg \min_{Y_0} \lambda \|Y_0\|_1 + \frac{\rho}{2} \left\| Y_0 - (X^{(j+1)} + U_0^{(j)}) \right\|_F^2 \quad (65)$$

$$\begin{aligned} Y_1^{(j+1)} = \arg \min_{Y_1} \frac{1}{2} \|WY_1\|_F^2 + \\ \frac{\rho}{2} \left\| Y_1 - (DX^{(j+1)} - S + U_1^{(j)}) \right\|_F^2 \end{aligned} \quad (66)$$

$$U_0^{(j+1)} = U_0^{(j)} + X^{(j+1)} - Y_0^{(j+1)} \quad (67)$$

$$U_1^{(j+1)} = U_1^{(j)} + DX^{(j+1)} - Y_1^{(j+1)}. \quad (68)$$

The functional minimised in Eq. (64) is of the same form as Eq. (13), and can be solved via the same frequency domain method, the solution to Eq. (65) is as in Eq. (16), and the solution to Eq. (66) is given by

$$(W^T W + \rho I) Y_1 = \rho (DX^{(j+1)} - S + U_1^{(j)}). \quad (69)$$

The other method for solving Eq. (61) involves appending an impulse filter to the dictionary and solving the problem in a way that constrains the coefficient map corresponding to this filter to be zero where the mask is unity, and to be unconstrained where the mask is zero [31], [15]. Both approaches provide very similar performance [15], the major difference being that the former is a bit more complicated to implement, while the latter is restricted to addressing problems where W has only zero or one entries. We will use the former mask decoupling approach for the experiments reported here since it does not require any restrictions on the form of W .

B. Dictionary Update

The dictionary update requires solving the problem

$$\arg \min_{\mathbf{d}} \frac{1}{2} \left\| W(X\mathbf{d} - \mathbf{s}) \right\|_2^2 + \iota_{C_{\text{PN}}}(\mathbf{d}). \quad (70)$$

Algorithms for solving this problem are discussed in the following section.

⁶For simplicity, the notation presented here assumes a fixed mask W across all columns of DX and S , but the algorithm is easily extended to handle a different W_k for each column k .

V. MASKED DICTIONARY UPDATE ALGORITHMS

A. Block-Constraint ADMM

Problem Eq. (70) can be solved via the splitting [9]

$$\begin{aligned} \arg \min_{\mathbf{d}} \frac{1}{2} \|W\mathbf{g}_1\|_2^2 + \iota_{C_{\text{PN}}}(\mathbf{g}_0) \\ \text{s.t. } \mathbf{g}_0 = \mathbf{d} \quad \mathbf{g}_1 = X\mathbf{d} - \mathbf{s}, \end{aligned} \quad (71)$$

where the constraint can also be written as

$$\begin{pmatrix} \mathbf{g}_0 \\ \mathbf{g}_1 \end{pmatrix} = \begin{pmatrix} I \\ X \end{pmatrix} \mathbf{d} - \begin{pmatrix} 0 \\ \mathbf{s} \end{pmatrix}. \quad (72)$$

This problem has the same structure as Eq. (62), the only difference being the replacement of the ℓ_1 norm with the indicator function of the constraint set. Hence, the ADMM iterations are largely the same as Eq. (64)-(68), except that the ℓ_1 norm in Eq. (65) is replaced with the indicator function of the constraint set, and that the step corresponding to Eq. (64) is more computationally expensive to solve, just as Eq. (30) is more expensive than Eq. (13).

B. Extended Consensus Framework

In this section we re-use the variant notation introduced in Sec. III-B. The masked dictionary update Eq. (70) can be solved via a hybrid of the mask decoupling and ADMM consensus approaches, which can be formulated as

$$\begin{aligned} \arg \min_{\mathbf{d}_c} \frac{1}{2} \|W\mathbf{g}_1\|_2^2 + \iota_{C_{\text{PN}}}(\mathbf{g}_0) \\ \text{s.t. } E\mathbf{g}_0 = \mathbf{d} \quad \mathbf{g}_1 = X\mathbf{d} - \mathbf{s}, \end{aligned} \quad (73)$$

where the constraint can also be written as

$$\begin{pmatrix} I \\ X \end{pmatrix} \mathbf{d} + \begin{pmatrix} -E & 0 \\ 0 & -I \end{pmatrix} \begin{pmatrix} \mathbf{g}_0 \\ \mathbf{g}_1 \end{pmatrix} = \begin{pmatrix} 0 \\ \mathbf{s} \end{pmatrix}, \quad (74)$$

or, expanding the block components of \mathbf{d} , \mathbf{g}_1 , and \mathbf{s} ,

$$\begin{pmatrix} I & 0 & \dots \\ 0 & I & \dots \\ \vdots & \vdots & \ddots \\ X_0 & 0 & \dots \\ 0 & X_1 & \dots \\ \vdots & \vdots & \ddots \end{pmatrix} \begin{pmatrix} \mathbf{d}_0 \\ \mathbf{d}_1 \\ \vdots \end{pmatrix} - \begin{pmatrix} \mathbf{g}_0 \\ \mathbf{g}_0 \\ \vdots \\ \mathbf{g}_{1,0} \\ \mathbf{g}_{1,1} \\ \vdots \end{pmatrix} = \begin{pmatrix} 0 \\ 0 \\ \vdots \\ \mathbf{s}_0 \\ \mathbf{s}_1 \\ \vdots \end{pmatrix}. \quad (75)$$

The corresponding ADMM iterations are

$$\begin{aligned} \mathbf{d}^{(j+1)} = \arg \min_{\mathbf{d}} \frac{\rho}{2} \left\| X\mathbf{d} - (\mathbf{g}_1^{(j)} + \mathbf{s} - \mathbf{h}_1^{(j)}) \right\|_2^2 + \\ \frac{\rho}{2} \left\| \mathbf{d} - (E\mathbf{g}_0^{(j)} - \mathbf{h}_0^{(j)}) \right\|_2^2 \end{aligned} \quad (76)$$

$$\mathbf{g}_0^{(j+1)} = \arg \min_{\mathbf{g}_0} \iota_{C_{\text{PN}}}(\mathbf{g}_0) + \frac{\rho}{2} \left\| E\mathbf{g}_0 - (\mathbf{d}^{(j+1)} + \mathbf{h}_0^{(j)}) \right\|_2^2 \quad (77)$$

$$\begin{aligned} \mathbf{g}_1^{(j+1)} = \arg \min_{\mathbf{g}_1} \frac{1}{2} \|W\mathbf{g}_1\|_2^2 + \\ \frac{\rho}{2} \left\| \mathbf{g}_1 - (X\mathbf{d}^{(j+1)} - \mathbf{s} + \mathbf{h}_1^{(j)}) \right\|_2^2 \end{aligned} \quad (78)$$

$$\mathbf{h}_0^{(j+1)} = \mathbf{h}_0^{(j)} + \mathbf{d}^{(j+1)} - E\mathbf{g}_0^{(j+1)} \quad (79)$$

$$\mathbf{h}_1^{(j+1)} = \mathbf{h}_1^{(j)} + X\mathbf{d}^{(j+1)} - \mathbf{g}_1^{(j+1)}. \quad (80)$$

Steps Eq. (76), (77), and (79) have the same form, and can be solved in the same way, as steps Eq. (42), (43),

and (44) respectively of the ADMM algorithm in Sec. III-B, and steps Eq. (78) and (80) have the same form, and can be solved in the same way, as the corresponding steps in the ADMM algorithm of Sec. V-A.

C. FISTA

Problem Eq. (70) can be solved via FISTA as described in Sec. III-D, but the calculation of the gradient term is complicated by the presence of the spatial mask. This difficulty can be handled by transforming back and forth between spatial and frequency domains so that the convolution operations are computed efficiently in the frequency domain, while the masking operation is computed in the spatial domain, i.e.

$$F\left(\nabla_{\mathbf{d}}\left(\frac{1}{2}\|W(X\mathbf{d}-\mathbf{s})\|_2^2\right)\right) = \hat{X}^H F\left(W^T W F^{-1}(\hat{X}\hat{\mathbf{d}}-\hat{\mathbf{s}})\right), \quad (81)$$

where F and F^{-1} represent the DFT and inverse DFT transform operators, respectively.

VI. RESULTS

In this section we compare the computational performance of the various approaches that have been discussed, carefully selecting optimal parameters for each algorithm to ensure a fair comparison.

A. Dictionary Learning Algorithms

Before proceeding to performance results, we summarize the dictionary learning algorithms that will be compared. Instead of using the complete dictionary learning algorithm proposed in each prior work, we consider the primary contribution of these works to be in the dictionary update method, which is incorporated into the CDL algorithm structure that was demonstrated in [21] to be most effective: auxiliary variable coupling with a single iteration for each subproblem⁷ before alternating. Since the sparse coding stages are the same, the algorithm naming is based on the dictionary update algorithms.

The following CDL algorithms are considered for problem Eq. (1) without a spatial mask

Conjugate Gradient (CG) The CDL algorithm is as proposed in [5].

Iterated Sherman-Morrison (ISM) The CDL algorithm is as proposed in [5].

Spatial Tiling (Tiled) The CDL algorithm uses the dictionary update proposed in [22], but the more effective variable coupling and alternation strategy discussed in [21].

ADMM Consensus (Cns) The CDL algorithm uses the dictionary update proposed in [22], but the more effective variable coupling and alternation strategy discussed in [21].

ADMM Consensus in Parallel (Cns-P) The algorithm is the same as Cns, but with a parallel implementation of

both the sparse coding and dictionary update stages⁸. All steps of the CSC stage are completely parallelizable in the training image index k , as are the \mathbf{d} and \mathbf{h} steps of the dictionary update, the only synchronization point being in the \mathbf{g} step, Eq. (48), where all the independent dictionary estimates are averaged to update the consensus variable that all the processes share.

3D (3D) The CDL algorithm uses the dictionary update proposed in [22], but the more effective variable coupling and alternation strategy discussed in [21].

FISTA (FISTA) Not previously considered for this problem.

The following dictionary learning algorithms are considered for problem Eq. (60) with a spatial mask

Conjugate Gradient (M-CG) Not previously considered for this problem.

Iterated Sherman-Morrison (M-ISM) The CDL algorithm is as proposed in [15].

Extended Consensus (M-Cns) The CDL algorithm is based on a new dictionary update constructed as a hybrid of the dictionary update methods proposed in [9] and [22].

FISTA (M-FISTA) Not previously considered for this problem.

In addition to the algorithms listed above, we considered the Stochastic Averaging ADMM (SA-ADMM) [32], as proposed for CDL in [10]. Our implementation of a CDL algorithm based on this method was found to have promising computational cost per iteration, but its convergence was not competitive with some of the other methods considered here. However, since there are a number of algorithm details that are not provided in [10] (CDL is not the primary topic of that work), it is possible that our implementation omits some critical components. These results are therefore not included here in order to avoid making an unfair comparison.

We do not compare with the dictionary learning algorithm in [7] because the algorithms of both [9] and [22] were both reported to be substantially faster. Similarly, we do not compare with the dictionary learning algorithm in [9] because the alternative approach considered in [15] was found to be faster, and to avoid the very high memory requirements, resulting from the strategy of caching matrix factorizations, that make it difficult to apply this method to training images of even moderate size.

Due to space limitations we do not discuss multi-channel CDL [33] here, but it is worth noting that all of the algorithms proposed here can be extended to multi-channel CDL, and our implementations of all of these algorithms, included in the SPORCO software package [34], [35], support this extension.

B. Experiments

We use training sets (one of each size) of 5, 10, 20, and 40 images. These sets are nested in the sense that all images in a set are also present in all the larger sets. The parent set of 40 images consists of grayscale images of size 256×256

⁷In some cases, slightly better time performance can be obtained by performing a few iterations of the sparse coding update followed by a single dictionary update, but we do not consider this complication here.

⁸Šorel and Šroubek [22] observe that the ADMM Consensus problem is inherently parallelizable [16, Ch. 7], but do not actually implement the corresponding CDL algorithm in parallel form to allow the resulting computational gain to be quantified empirically.

pixels, cropped and rescaled from a set of images selected from the MIRFLICKR-1M dataset⁹ [36]. An additional set of 20 images, of the same size and from the same source, is used as a test set to allow comparison of generalization performance, taking into account possible differences in overfitting effects between the different methods. These 8 bit greyscale images are divided by 255 so that pixel values are within the interval $[0,1]$, and are highpass filtered (a common approach for convolutional sparse representations [37], [38], [5][39, Sec. 3]) by subtracting a lowpass component computed by Tikhonov regularization with a gradient term [35, pg. 3], with regularization parameter $\lambda = 5.0$.

All the results reported here were computed using the Python implementation of the SPORCO library [34], [35] on a Linux workstation equipped with two Xeon E5-2690V4 CPUs.

C. Optimal Penalty Parameters

To ensure a fair comparison between the methods, the optimal penalty parameters for each method and training image set were selected via a grid search, of CDL functional values obtained after 100 iterations, over (ρ, σ) values for the ADMM dictionary updates, and over (ρ, L) values for the FISTA dictionary updates. The grid resolutions were

- ρ 10 logarithmically spaced points in $[10^{-1}, 10^4]$
- σ 15 logarithmically spaced points in $[10^{-2}, 10^5]$
- L 15 logarithmically spaced points in $[10^1, 10^5]$

The best set of (ρ, σ) or (ρ, L) for each method i.e. the ones yielding the lowest value of the CDL functional at 100 iterations, was selected as a center for a finer grid search, of CDL functional values obtained after 200 iterations, with 10 logarithmically spaced points in $[0.1\rho_{\text{center}}, 10\rho_{\text{center}}]$ and 10 logarithmically spaced points in $[0.1\sigma_{\text{center}}, 10\sigma_{\text{center}}]$ or 10 logarithmically spaced points in $[0.1L_{\text{center}}, 10L_{\text{center}}]$. The optimal parameters for each method were taken as those yielding the lowest value of the CDL functional at 200 iterations in this finer grid. This procedure was repeated for sets of 5, 10 and 20 images. As an indication of the sensitivities of the different methods to their parameters, results for the coarse grid search for the 20 image set can be found in Sec. III in the Supplementary Material.

Since computing grid searches for the case of $K = 40$ is very expensive, we extrapolated the optimal parameters found in the smaller sized problems and performed a coarser resolution grid search around those values. We used 3 logarithmically spaced points in $[0.5\rho_{\text{center}}, 2\rho_{\text{center}}]$ and 3 logarithmically spaced points in $[0.5\sigma_{\text{center}}, 2\sigma_{\text{center}}]$ or 3 logarithmically spaced points in $[0.5L_{\text{center}}, 2L_{\text{center}}]$ and selected the (ρ, σ) or (ρ, L) combination yielding the lowest value of the CBPDN functional at 200 iterations as the optimal parameters.

The optimal parameters determined via these grid searches are summarized in Table I.

⁹The actual image data contained in this dataset is of very low resolution since the dataset is primarily targeted at image classification tasks. The high resolution images from which those used here were derived were obtained by downloading the original images that were used to derive the MIRFLICKR-1M images.

TABLE I
DICTIONARY LEARNING: OPTIMAL PARAMETERS FOUND BY GRID SEARCH.

Method	K	Parameter		Method	Parameter	
		ρ	σ		ρ	σ
CG	5	3.59	4.08	M-CG	3.59	5.99
	10	3.59	12.91		3.59	7.74
	20	2.15	24.48		2.15	7.74
	40	2.56	62.85		2.49	11.96
ISM	5	3.59	4.08	M-ISM	3.59	5.99
	10	3.59	12.91		3.59	7.74
	20	2.15	24.48		2.15	7.74
	40	2.56	62.85		2.49	11.96
Tiled	5	3.59	7.74			
	10	3.59	12.91			
	20	3.59	40.84			
	40	3.59	72.29			
Cns	5	3.59	1.29	M-Cns	3.59	1.13
	10	3.59	1.29		3.59	0.68
	20	3.59	2.15		3.59	1.13
	40	3.59	1.08		3.59	1.01
3D	5	3.59	7.74			
	10	3.59	12.91			
	20	3.59	40.84			
	40	3.59	72.29			
			L			
FISTA	5	3.59	48.14			
	10	3.59	92.95			
	20	3.59	207.71			
	40	3.59	400.00			

D. Performance Comparisons

We compare the performance of the methods in learning a dictionary of 64 filters of size 8×8 for sets of 5, 10, 20 and 40 images, setting the sparsity parameter $\lambda = 0.1$, and using the parameters determined by the grid searches for each method. To avoid complicating the comparisons, we used fixed penalty parameters ρ and σ without any adaptation methods [5, Sec. III.D], and did not apply relaxation methods [16, Sec. 3.4.3][5, Sec. III.D] in any of the ADMM algorithms. Performance is compared in Figs. 1 – 3 in terms of the convergence rate, with respect to both iterations and computation time, of the CDL functional. The time scaling of all the methods is summarized in Fig. 7(a).

For the $K = 5$ case, all the methods have quite similar performance in terms of functional value convergence with respect to iterations. For the larger training set sizes, CG and ISM have somewhat better performance with respect to iterations, but ISM has very poor performance with respect to time. CG has substantially better time scaling, depending on the relative residual tolerance. We ran our experiments for CG with a fixed tolerance of 10^{-3} , resulting in computation times that are comparable with those of the other methods. A smaller tolerance leads to better convergence with respect to iterations, but substantially worse time performance.

Both parallel (Cns-P) and regular consensus (Cns) have the same evolution of the CBPDN functional, Eq. (5), with respect to iterations, but the former requires much less computation time, and is the fastest method overall. Moreover, parallel

consensus yields almost ideal speedups, with some overhead for $K = 5$, but scaling linearly for $K \in [10, 40]$, and with very competitive computation times. FISTA is also very competitive, achieving good results in less time than any of the other serial methods, and almost matching the time scaling with K of parallel consensus (see Fig. 7(a)).

As expected from the relationship established in Sec. III-C, 3D behaves similarly to ADMM consensus, but has a larger memory footprint. The spatial tiling method (Tiled), on the other hand, tends to have slower convergence with respect to both iterations and time than the other methods. We do not further explore the performance of these methods since they do not provide substantial advantages over the other ones discussed.

All experiments with algorithms that include a spatial mask set the mask to the identity ($W = I$) to allow comparison with the performance of the algorithms without a spatial mask. Plots comparing the evolution of the masked CBPDN functional, Eq. (61), during 1000 iterations and problem sizes of $K \in \{5, 20, 40\}$ are displayed in Figs. 4 – 6, respectively. The time scaling of all the masked methods is summarized in Fig. 7(b).

It is clear that, despite the additional FFTs required for computing the masked version of the FISTA algorithm, this is a more time-efficient procedure than the mask decoupling ADMM variants. It is also clear that the hybrid mask decoupling/consensus dictionary update (M-Cns) yields a better convergence with iterations and competitive time scaling. While we have not implemented a parallel version of this method, the overall algorithm structure is sufficiently similar to that of the consensus dictionary update to support the conclusion that it would exhibit similar performance gains from parallelization, which would give it the best time performance of any of the methods considered for the CDL problem with mask decoupling.

In contrast with the corresponding mask-free variants, M-CG and M-ISM have worse performance in terms of both time and iterations. This suggests that M-CG requires a value for the relative residual tolerance smaller than 10^{-3} to produce good results, but this would be at the expense of much longer computation times.

With the exception of CG, for which the cost of computing the masked version increases for $K \geq 20$, the computation time for the masked versions is only slightly worse than the mask-free variants (Fig. 7). In general, using the masked versions leads to a marginal decrease in convergence rate with respect to iterations and a small increase in computation time.

E. Evaluation on the Test Set

To enable a comparison that takes into account any possible differences in overfitting and generalization properties of the dictionaries learned by the different methods, we ran experiments over a 20 image test set that was not used during learning. For all the methods discussed, we saved the dictionaries at 50 iteration intervals (including the final one obtained at 1000 iterations) while training. These dictionaries were used to sparse code the images in the test set and report

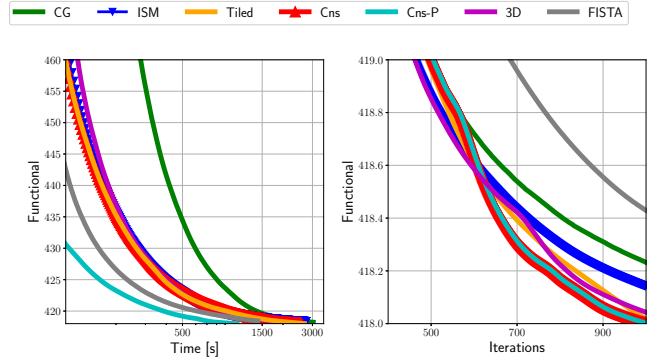


Fig. 1. Dictionary Learning ($K = 5$): A comparison on sets of $K = 5$ images of the decay of the value of the CBPDN functional Eq. (5) with respect to run time and iterations. ISM, Tiled, Cns and 3D overlap in the time plot, and Cns and Cns-P overlap in the iterations plot.

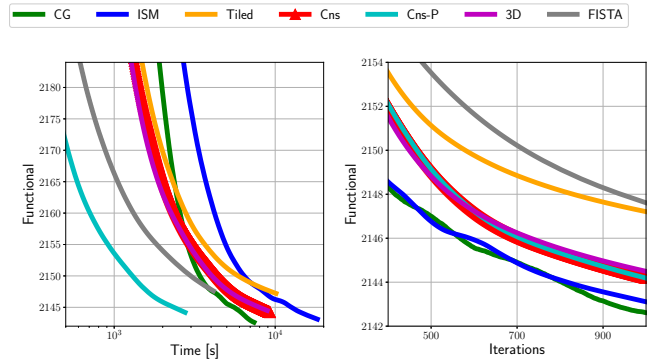


Fig. 2. Dictionary Learning ($K = 20$): A comparison on sets of $K = 20$ images of the decay of the value of the CBPDN functional Eq. (5) with respect to run time and iterations. Cns and 3D overlap in the time plot, and Cns, Cns-P and 3D overlap in the iterations plot.

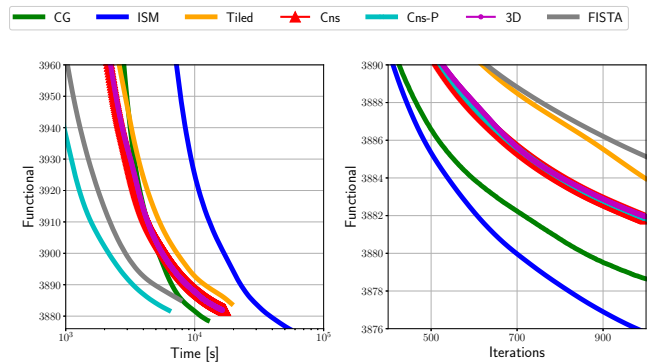


Fig. 3. Dictionary Learning ($K = 40$): A comparison on sets of $K = 40$ images of the decay of the value of the CBPDN functional Eq. (5) with respect to run time and iterations. Cns and 3D overlap in the time plot, and Cns, Cns-P and 3D overlap in the iterations plot.

the evolution of the CBPDN functional for $\lambda = 0.1$. Results for the dictionaries learned while training with $K = 20$ and $K = 40$ images are shown in Figs. 8 and 9 respectively, and corresponding results for the algorithms with a spatial mask are shown in Figs. 10 and 11 respectively. Note that the time axis in these plots refers to the run time of the dictionary learning code used to generate the relevant dictionary, and *not*

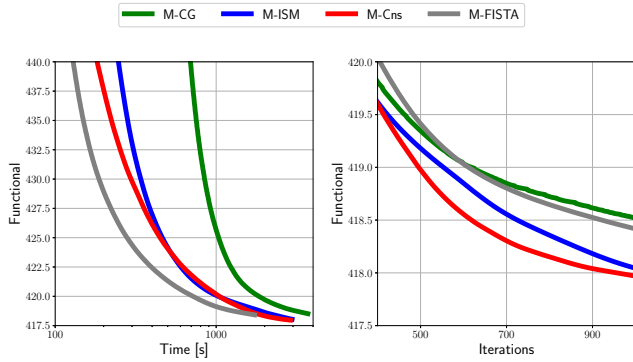


Fig. 4. Dictionary Learning with Spatial Mask ($K = 5$): A comparison on sets of $K = 5$ images of the decay of the value of the masked CBPDN functional Eq. (61) with respect to run time and iterations for masked versions of the algorithms.

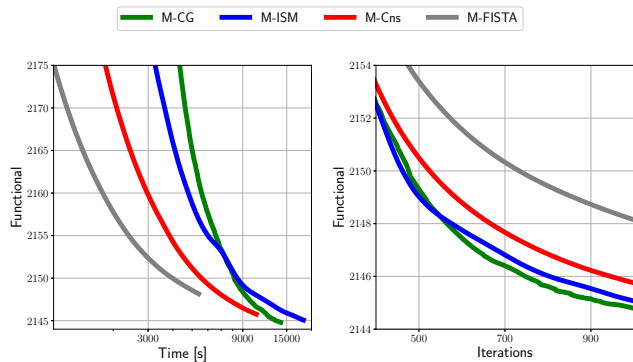


Fig. 5. Dictionary Learning with Spatial Mask ($K = 20$): A comparison on sets of $K = 20$ images of the decay of the value of the masked CBPDN functional Eq. (61) with respect to run time and iterations for masked versions of the algorithms.

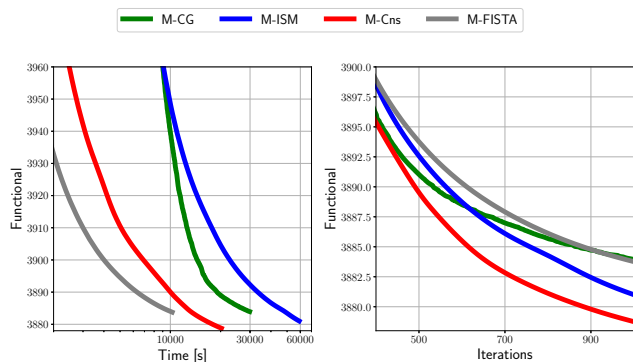
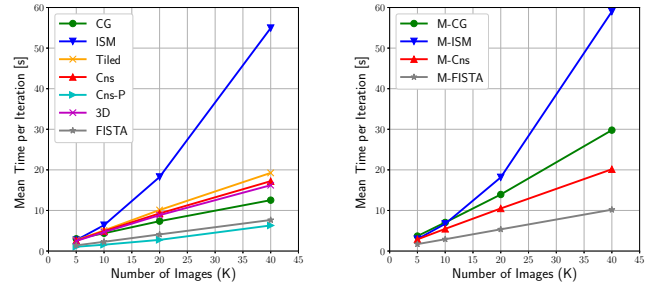


Fig. 6. Dictionary Learning with Spatial Mask ($K = 40$): A comparison on sets of $K = 40$ images of the decay of the value of the masked CBPDN functional Eq. (61) with respect to run time and iterations for masked versions of the algorithms.

to the run time of the sparse coding on the test set. Therefore, at any given instant we know which method is giving the best test performance, which would be particularly important when learning a dictionary subject to a run time constraint.

As expected, independent of the method, the dictionaries obtained for training with 40 images exhibit better performance than the ones trained with 20 images. Overall, performance



(a) Without Spatial Mask

(b) With Spatial Mask

Fig. 7. Comparison of time per iteration for the dictionary learning methods for sets of 5, 10, 20 and 40 images.

on training is a good predictor of performance in testing, which suggests that the functional value on a sufficiently large training set is a reliable indicator of dictionary quality.

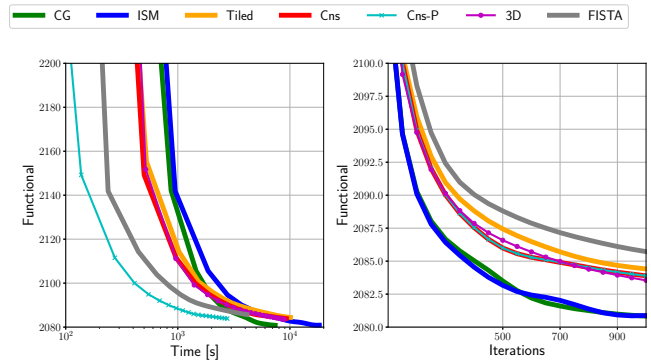


Fig. 8. Evolution of the CBPDN functional Eq. (5) for the test set using the partial dictionaries obtained when training for $K = 20$ images. Tiled, Cns and 3D overlap in the time plot, and Cns and Cns-P overlap in the iterations plot.

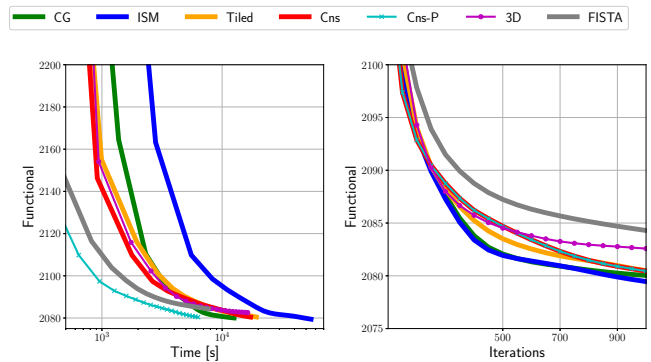


Fig. 9. Evolution of the CBPDN functional Eq. (5) for the test set using the partial dictionaries obtained when training for $K = 40$ images. Tiled, Cns and 3D have a large overlap in the time plot, and Cns and Cns-P overlap in the iterations plot.

F. Penalty Parameter Selection

The grid searches performed for determining optimal parameters ensure a fair comparison between the methods, but

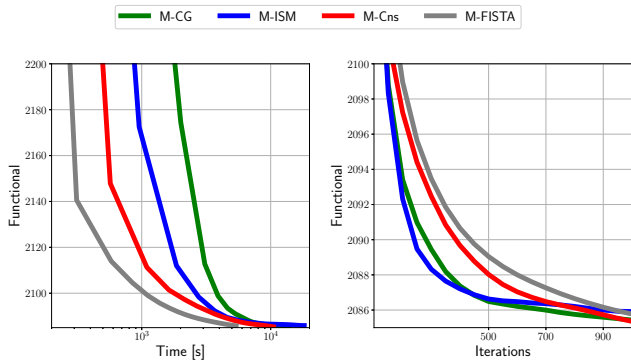


Fig. 10. Evolution of the masked CBPDN functional Eq. (61) for the test set using the partial dictionaries obtained when training for $K = 20$ images for masked versions of the algorithms.

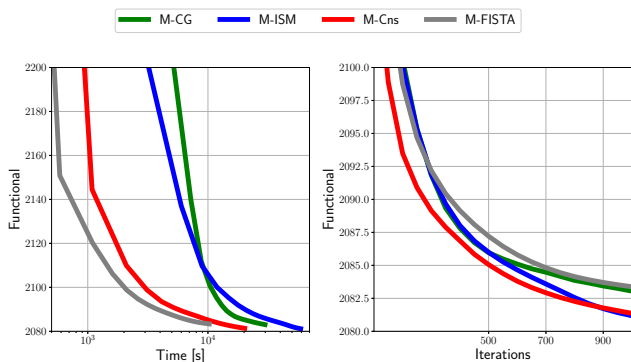


Fig. 11. Evolution of the masked CBPDN functional Eq. (61) for the test set using the partial dictionaries obtained when training for $K = 40$ images for masked versions of the algorithms.

they are not convenient as a general approach to parameter selection. In this section we show that it is possible to construct heuristics that provide reliable parameter selections for the best performing CDL methods considered here.

1) *Parameter Scaling Properties:* In Sec. SIII in the Supplementary Material we derive the scaling properties with respect to K of the different algorithms discussed here by considering the simplified case in which the training set size is changed by replication of the same training data. For the CDL problem without a spatial mask, these scaling properties are derived for the sparse coding problem and for the different dictionary learning updates: ADMM with equality constraint, ADMM with consensus constraint and FISTA. These results show that the scaling of the penalty parameter ρ for the convolutional sparse coding is $\mathcal{O}(1)$, the scaling of the penalty parameter σ for the dictionary learning update is $\mathcal{O}(K)$ for the ADMM with equality constraint and $\mathcal{O}(1)$ for consensus ADMM, and the scaling of the step size L for FISTA is $\mathcal{O}(K)$. Analytic derivations for Tiled and 3D methods do not lead to a simple scaling relationship, and are not included.

Likewise, for the masked versions we derive the scaling properties of the parameters for the sparse coding, dictionary learning with block-constraint ADMM and dictionary learning with consensus framework. The scaling of the penalty parameter ρ for the masked version of the convolutional sparse

coding is $\mathcal{O}(1)$, the scaling of the penalty parameter σ for the dictionary learning update in the masked consensus framework is $\mathcal{O}(1)$, while there is no simple rule of the σ scaling in the block-constraint ADMM of Sec. V-A.

2) *Penalty Parameter Sensitivity:* While the analytic derivations of parameter scaling properties represent a useful guide to estimating optimal parameters for a training set given those of a training set of a different size, they do not provide any indication of the stability of these parameters across different training subsets. We therefore provide an empirical evaluation of the sensitivity of the penalty parameters across different training image subsets, for the most effective method in each representative class in the dictionary learning update: conjugate gradient (for ADMM with equality constraint), consensus (for ADMM with consensus constraint) and FISTA (for iterative gradient descent). For masked versions, we include an empirical evaluation for the hybrid consensus method, which, besides M-FISTA, is the only one with a simple parameter scaling behaviour. We do not compute a separate empirical sensitivity analysis for the masked version of FISTA because it has the same functional evolution as the mask-free version for the identity mask $W = I$.

For each training set size $K \in \{5, 10, 20\}$ we randomly selected 20 different image subsets from the 40 image training set. We performed grid searches, of CDL functional values obtained after 100 iterations, over (ρ, σ) values for the ADMM dictionary updates, and over (ρ, L) values at 200 iterations for the FISTA dictionary updates. We used the following resolutions: for CG, 10 logarithmically spaced points in $[1, 10^3]$ for ρ and σ ; for Cns, 10 logarithmically spaced points in $[1, 10^3]$ for ρ and 10 logarithmically spaced points in $[10^{-1}, 10^2]$ for σ ; and for FISTA, 10 logarithmically spaced points in $[1, 10^{1.3}]$ for ρ , 10 logarithmically spaced points in $[10^{1.3}, 10^{2.7}]$ for L with $K \in \{5, 10\}$ and 10 logarithmically spaced points in $[10^{1.5}, 10^3]$ for L with $K = 20$. The ranges of these were set in agreement with the results obtained in the first grid searches. We normalized the results for each subset by dividing by the minimum of the functional for that subset, and computed statistics over these normalized values. These statistics are reported as box plots (median, quartiles and spread) for all the representative methods in Sec. SIV in the Supplementary Material.

TABLE II
PENALTY PARAMETER SELECTION GUIDELINES

Parameter	Method	Rule
ρ	All	$\rho = 5$
σ	CG, ISM	$\sigma = K$
	Cns, M-Cns	$\sigma = 1$
L	FISTA	$L = 12K$

Fig. 12 displays a summary of the scaling of the penalty parameters. For each of the problem sizes K , we computed the median of the normalized CDL values for each point in the search grids of the random subsets, and we plotted the penalty parameters corresponding to the minima of the median. We also determined the part of the grid that is in the 2% of the minima of the normalized CDL values, and plotted it as

spread bars per K . The figure includes plots for ρ and σ for CG, consensus and consensus with spatial mask; and ρ and L for FISTA. Results for ISM are the same as for CG and are not shown. For the methods that lead to a simple scaling relationship (for which analytic derivations are provided in the Supplementary Material), we combined the theoretical expected scaling with the results of the experimental sensitivity analysis, to construct guidelines for setting the parameters. These guidelines are plotted in black, and are also summarized in Table II.

Note that L , the inverse of the gradient step size in FISTA, has to be greater than or equal to the Lipschitz constant of the gradient of the functional to guarantee convergence of the algorithm, but this constant is not always computable [30]. Empirically, we find that smaller values of L yield a worse final value of the CBPDN functional, and therefore, very skewed sensitivity plots, with smooth changes of the functional above the optimal value, but large jumps below it, and medians closer to the minima of the 2% interval. A similar but less marked behavior can be seen in ρ , the penalty parameter for the CSC problem, with slower degradation for values above the optimal value, more rapid degradation for values below the optimum, and medians closer to the minima of the 2% interval.

The parameter selection guidelines presented in this section should only be expected to be reliable for training data with similar characteristics to those used in our experiments, i.e. natural images scaled to pixel values in the range $[0, 1]$ and pre-processed via the same or similar lowpass filtering. Nevertheless, since the scaling properties derived in Sec. SIII of the Supplementary Material remain valid, it is reasonable to expect that similar heuristics, albeit with different parameters (e.g. constants in the case of $\mathcal{O}(1)$ scaling and slopes in the case of $\mathcal{O}(K)$ scaling), would hold for different image content or different choices of lowpass filtering.

VII. CONCLUSIONS

Our results indicate that two distinct approaches to the dictionary update problem provide the leading CDL algorithms. In a serial processing context, the FISTA dictionary update proposed here outperforms all other methods, including consensus, for CDL with and without a spatial mask. This may seem surprising when considering that ADMM outperforms FISTA on the CSC problem, but is easily understood when taking into account the critical difference between the linear systems that need to be solved when tackling the CSC and convolutional dictionary update problems via proximal methods such as ADMM and FISTA. In the case of CSC, the major linear system to be solved has a frequency domain structure that allows very efficient solution via the Sherman-Morrison formula, providing an advantage to ADMM. In contrast, except for the $K = 1$ case, there is no such highly efficient solution for the convolutional dictionary update, giving an advantage to methods such as FISTA that employ gradient descent steps rather than solving the linear system.

In a parallel processing context, the consensus dictionary update proposed in [22] used together with the alternative

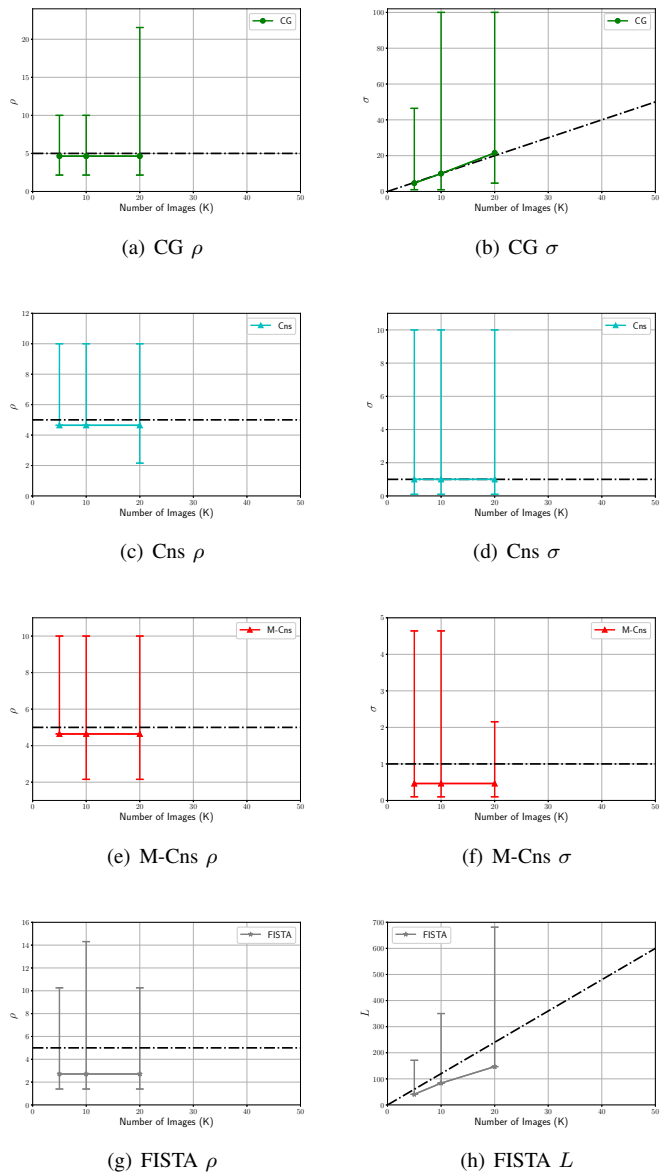


Fig. 12. Scaling of penalty parameters. Lines in color show the minima of the median of the normalized values of the CDL functional, while bars correspond to values of the parameters for which their functional value is in the 2% of the normalized minima. Practical rules combining the analytic derivations with an experimental sensitivity analysis are plotted in black for representative methods with simple scaling relationships.

CDL algorithm structure proposed in [21] leads to the CDL algorithm with the best time performance for the mask-free CDL problem, and we expect that a parallel implementation of the hybrid mask decoupling/consensus dictionary update proposed here will provide the best time performance for the masked CDL problem. It is interesting to note that, despite the clear suitability of the ADMM consensus framework for the convolutional dictionary update problem, a parallel implementation is essential to outperforming other methods; in a serial processing context it is significantly outperformed by the FISTA dictionary update, and even the CG method is competitive with it.

We have also demonstrated that the optimal algorithm

parameters for the leading methods considered here tend to be quite stable across different training sets of similar type, and have provided reliable heuristics for selecting parameters that provide good performance.

In the interest of reproducible research, software implementations of the algorithms considered here will be made publicly available as part of the SPORCO library [34], [35].

REFERENCES

- [1] J. Mairal, F. Bach, and J. Ponce, "Sparse modeling for image and vision processing," *Foundations and Trends in Computer Graphics and Vision*, vol. 8, no. 2-3, pp. 85–283, 2014. doi:10.1561/06000000058
- [2] M. A. T. Figueiredo, "Synthesis versus analysis in patch-based image priors," in *Proc. IEEE Int. Conf. Acoust. Speech Signal Process. (ICASSP)*, Mar. 2017, pp. 1338–1342. doi:10.1109/ICASSP.2017.7952374
- [3] M. S. Lewicki and T. J. Sejnowski, "Coding time-varying signals using sparse, shift-invariant representations," in *Adv. Neural Inf. Process. Syst. (NIPS)*, vol. 11, 1999, pp. 730–736.
- [4] M. D. Zeiler, D. Krishnan, G. W. Taylor, and R. Fergus, "Deconvolutional networks," in *Proc. IEEE Conf. Comp. Vis. Pat. Recog. (CVPR)*, Jun. 2010, pp. 2528–2535. doi:10.1109/cvpr.2010.5539957
- [5] B. Wohlberg, "Efficient algorithms for convolutional sparse representations," *IEEE Trans. Image Process.*, vol. 25, no. 1, pp. 301–315, Jan. 2016. doi:10.1109/TIP.2015.2495260
- [6] R. Chalasani, J. C. Principe, and N. Ramakrishnan, "A fast proximal method for convolutional sparse coding," in *Proc. Int. Joint Conf. Neural Net. (IJCNN)*, Aug. 2013. doi:10.1109/IJCNN.2013.6706854
- [7] H. Bristow, A. Eriksson, and S. Lucey, "Fast convolutional sparse coding," in *Proc. IEEE Conf. Comp. Vis. Pat. Recog. (CVPR)*, Jun. 2013, pp. 391–398. doi:10.1109/CVPR.2013.57
- [8] B. Wohlberg, "Efficient convolutional sparse coding," in *Proc. IEEE Int. Conf. Acoust. Speech Signal Process. (ICASSP)*, May 2014, pp. 7173–7177. doi:10.1109/ICASSP.2014.6854992
- [9] F. Heide, W. Heidrich, and G. Wetzstein, "Fast and flexible convolutional sparse coding," in *Proc. IEEE Conf. Comp. Vis. Pat. Recog. (CVPR)*, 2015, pp. 5135–5143. doi:10.1109/CVPR.2015.7299149
- [10] S. Gu, W. Zuo, Q. Xie, D. Meng, X. Feng, and L. Zhang, "Convolutional sparse coding for image super-resolution," in *Proc. IEEE Intl. Conf. Comput. Vis. (ICCV)*, Dec. 2015. doi:10.1109/ICCV.2015.212
- [11] Y. Liu, X. Chen, R. K. Ward, and Z. J. Wang, "Image fusion with convolutional sparse representation," *IEEE Signal Process. Lett.*, 2016. doi:10.1109/lsp.2016.2618776
- [12] H. Zhang and V. Patel, "Convolutional sparse coding-based image decomposition," in *British Mach. Vis. Conf. (BMVC)*, York, UK, Sep. 2016.
- [13] T. M. Quan and W.-K. Jeong, "Compressed sensing reconstruction of dynamic contrast enhanced MRI using GPU-accelerated convolutional sparse coding," in *IEEE Intl. Symp. Biomed. Imag. (ISBI)*, Apr. 2016, pp. 518–521. doi:10.1109/ISBI.2016.7493321
- [14] H. Zhang and V. M. Patel, "Convolutional sparse and low-rank coding-based rain streak removal," in *Proc. IEEE Winter Conference on Applications of Computer Vision (WACV)*, March 2017.
- [15] B. Wohlberg, "Boundary handling for convolutional sparse representations," in *Proc. IEEE Conf. Image Process. (ICIP)*, Phoenix, AZ, USA, Sep. 2016, pp. 1833–1837. doi:10.1109/ICIP.2016.7532675
- [16] S. Boyd, N. Parikh, E. Chu, B. Peleato, and J. Eckstein, "Distributed optimization and statistical learning via the alternating direction method of multipliers," *Foundations and Trends in Machine Learning*, vol. 3, no. 1, pp. 1–122, 2010. doi:10.1561/22000000016
- [17] J. Liu, C. Garcia-Cardona, B. Wohlberg, and W. Yin, "Online convolutional dictionary learning," in *Proc. IEEE Conf. Image Process. (ICIP)*, Sep. 2017, Accepted, arXiv:1706.09563.
- [18] K. Degraux, U. S. Kamilov, P. T. Boufounos, and D. Liu, "Online convolutional dictionary learning for multimodal imaging," 2017, arXiv:1706.04256.
- [19] Y. Wang, Q. Yao, J. T. Kwok, and L. M. Ni, "Online convolutional sparse coding," 2017, arXiv:1706.06972.
- [20] B. Kong and C. C. Fowlkes, "Fast convolutional sparse coding (FCSC)," University of California, Irvine, Tech. Rep., May 2014.
- [21] C. Garcia-Cardona and B. Wohlberg, "Subproblem coupling in convolutional dictionary learning," in *Proc. IEEE Conf. Image Process. (ICIP)*, Sep. 2017, Accepted. [Online]. Available: <http://brendt.wohlberg.net/publications/garcia-2017-subproblem.html>
- [22] M. Šorel and F. Šroubek, "Fast convolutional sparse coding using matrix inversion lemma," *Digital Signal Processing*, 2016. doi:10.1016/j.dsp.2016.04.012
- [23] M. S. C. Almeida and M. A. T. Figueiredo, "Deconvolving images with unknown boundaries using the alternating direction method of multipliers," *IEEE Trans. Image Process.*, vol. 22, no. 8, pp. 3074–3086, Aug. 2013. doi:10.1109/tip.2013.2258354
- [24] M. Jas, T. D. L. Tour, U. Şimşekli, and A. Gramfort, "Learning the morphology of brain signals using alpha-stable convolutional sparse coding," 2017, arXiv:1705.08006.
- [25] V. Pappayan, Y. Romano, J. Sulam, and M. Elad, "Convolutional dictionary learning via local processing," 2017, arXiv:1705.03239.
- [26] I. Y. Chun and J. A. Fessler, "Convolutional dictionary learning: Acceleration and convergence," 2017, arXiv:1707.00389.
- [27] S. S. Chen, D. L. Donoho, and M. A. Saunders, "Atomic decomposition by basis pursuit," *SIAM J. Sci. Comput.*, vol. 20, no. 1, pp. 33–61, 1998. doi:10.1137/S1064827596304010
- [28] K. Engan, S. O. Aase, and J. H. Husøy, "Method of optimal directions for frame design," in *Proc. IEEE Int. Conf. Acoust. Speech Signal Process. (ICASSP)*, vol. 5, 1999, pp. 2443–2446. doi:10.1109/icassp.1999.760624
- [29] M. V. Afonso, J. M. Bioucas-Dias, and M. A. T. Figueiredo, "An Augmented Lagrangian approach to the constrained optimization formulation of imaging inverse problems," *IEEE Trans. Image Process.*, vol. 20, no. 3, pp. 681–695, Mar. 2011. doi:10.1109/tip.2010.2076294
- [30] A. Beck and M. Teboulle, "A fast iterative shrinkage-thresholding algorithm for linear inverse problems," *SIAM Journal on Imaging Sciences*, vol. 2, no. 1, pp. 183–202, 2009. doi:10.1137/080716542
- [31] B. Wohlberg, "Endogenous convolutional sparse representations for translation invariant image subspace models," in *Proc. IEEE Conf. Image Process. (ICIP)*, Paris, France, Oct. 2014, pp. 2859–2863. doi:10.1109/ICIP.2014.7025578
- [32] L. W. Zhong and J. T. Kwok, "Fast stochastic alternating direction method of multipliers," in *Proc. Intl. Conf. Mach. Learn (ICML)*, Beijing, China, 2014, pp. 46–54.
- [33] B. Wohlberg, "Convolutional sparse representation of color images," in *Proc. IEEE Southwest Symp. Image Anal. Interp. (SSIAI)*, Santa Fe, NM, USA, Mar. 2016, pp. 57–60. doi:10.1109/SSIAI.2016.7459174
- [34] —, "Sparse Optimization Research CODE (SPORCO)," Software library available from <http://purl.org/brendt/software/sporco>, 2016.
- [35] —, "SPORCO: A Python package for standard and convolutional sparse representations," in *Proceedings of the 15th Python in Science Conference*, Austin, TX, USA, Jul. 2017, pp. 1–8.
- [36] M. J. Huiskes, B. Thomee, and M. S. Lew, "New trends and ideas in visual concept detection: The MIR Flickr retrieval evaluation initiative," in *Proc. International Conference on Multimedia Information Retrieval (MIR '10)*. ACM, 2010, pp. 527–536. doi:10.1145/1743384.1743475
- [37] K. Kavukcuoglu, P. Sermanet, Y. Boureau, K. Gregor, M. Mathieu, and Y. LeCun, "Learning convolutional feature hierarchies for visual recognition," in *Adv. Neural Inf. Process. Syst. (NIPS)*, 2010, pp. 1090–1098.
- [38] M. D. Zeiler, G. W. Taylor, and R. Fergus, "Adaptive deconvolutional networks for mid and high level feature learning," in *Proc. IEEE Int. Conf. Comp. Vis. (ICCV)*, Barcelona, Spain, Nov. 2011, pp. 2018–2025. doi:10.1109/iccv.2011.6126474
- [39] B. Wohlberg, "Convolutional sparse representations as an image model for impulse noise restoration," in *Proc. IEEE Image, Video Multi-dim. Signal Process. Workshop (IVMSP)*, Bordeaux, France, Jul. 2016. doi:10.1109/IVMSPW.2016.7528229

Convolutional Dictionary Learning: Supplementary Material

SI. INTRODUCTION

This document provides additional detail and results that were omitted from the main document due to space restrictions.

SII. PENALTY PARAMETER GRID SEARCH

The penalty parameter grid searches discussed in Sec. VI-C in the main text generate 2D surfaces representing the CDL functional value after a fixed number of iterations, plotted against the parameters for the sparse coding and dictionary update components of the dictionary learning algorithm. The surfaces corresponding to the coarse grids for the set of 20 training images are shown here in Figs. S1 – S3.

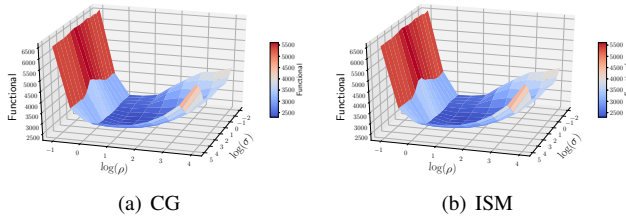


Fig. S1. Grid search surfaces for conjugate gradient (CG) and Iterated Sherman-Morrison (ISM) algorithms with $K = 20$. Each surface represents the value of the CBPDN functional (Eq. (3) in the main document) after 100 iterations obtained for different parameters ρ and σ .

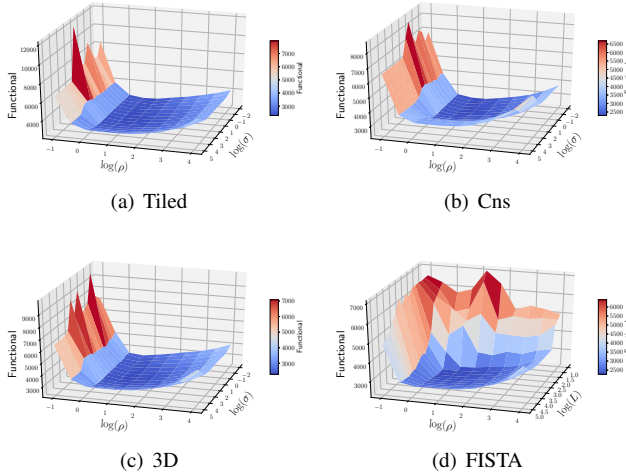


Fig. S2. Grid search surfaces for spatial tiling (Tiled), consensus (Cns), frequency domain consensus (3D) and FISTA algorithms with $K = 20$. Each surface represents the value of the CBPDN functional (Eq. (3) in the main document) after 100 iterations obtained for different parameters ρ and σ .

SIII. ANALYTIC DERIVATION OF PENALTY PARAMETER SCALING

In order to estimate the scaling properties of the algorithm parameters with respect to the training set size K , we consider the case in which the training set size is changed by replication

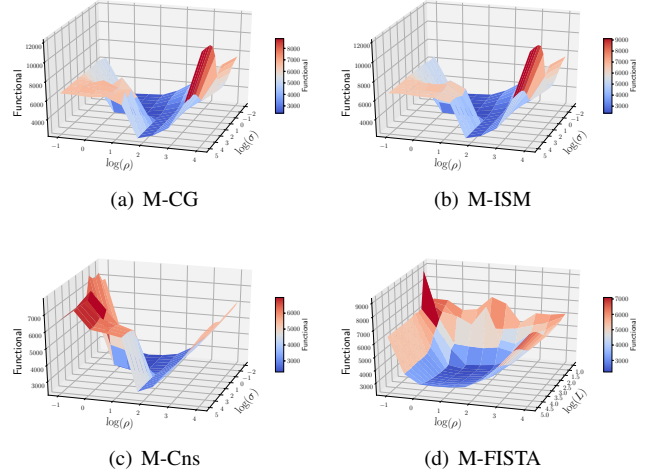


Fig. S3. Grid search surfaces for masked conjugate gradient (M-CG), masked iterated Sherman-Morrison (M-ISM), masked consensus (M-Cns) and masked FISTA (M-FISTA) algorithms with $K = 20$. Each surface represents the value of the masked CBPDN functional (Eq. (61) in the main document) after 100 iterations obtained for different parameters ρ and σ (or L for FISTA).

of the same data. By removing the complexities associated with the characteristics of individual images, this simplified scenario allows analytic evaluation of the conditions required to keep the same penalty level when the set size K is changed. In practice, when changing K involves introducing different training images, we cannot expect that these scaling properties will hold exactly, but they represent the best possible estimate that depends only on K and not on the properties of the training images themselves.

The following properties of the Frobenius norm, ℓ_2 norm, and ℓ_1 norm play an important role in these derivations:

$$\| \begin{pmatrix} \mathbf{x} & \mathbf{y} \end{pmatrix} \|_F^2 = \|\mathbf{x}\|_2^2 + \|\mathbf{y}\|_2^2 \quad (\text{S1})$$

$$\| \begin{pmatrix} \mathbf{x} & \mathbf{y} \end{pmatrix} \|_1 = \|\mathbf{x}\|_1 + \|\mathbf{y}\|_1. \quad (\text{S2})$$

A. ADMM Sparse Coding

The augmented Lagrangian for the ADMM solution to CSC problem Eq. (7) in the main document is

$$L_\rho(X, Y, U) = \frac{1}{2} \|DX - S\|_F^2 + \lambda \|Y\|_1 + \frac{\rho}{2} \|X - Y + U\|_F^2, \quad (\text{S3})$$

where we omit the final term $-\frac{\rho}{2} \|U\|_F^2$, which does not effect the minimizer of this functional. For $K = 1$ we have $S_1 = \mathbf{s}$, $X_1 = \mathbf{x}$, $Y_1 = \mathbf{y}$, and $U_1 = \mathbf{u}$. If we construct the $K = 2$ case by replicating the training data, we have $S_2 = \begin{pmatrix} \mathbf{s} & \mathbf{s} \end{pmatrix}$, $X_2 = \begin{pmatrix} \mathbf{x} & \mathbf{x} \end{pmatrix}$, $Y_2 = \begin{pmatrix} \mathbf{y} & \mathbf{y} \end{pmatrix}$, and $U_2 = \begin{pmatrix} \mathbf{u} & \mathbf{u} \end{pmatrix}$, and

the augmented Lagrangian is

$$\begin{aligned}
L_\rho(X_2, Y_2, U_2) &= \frac{1}{2} \|DX_2 - S_2\|_F^2 + \lambda \|Y_2\|_1 + \\
&\quad \frac{\rho}{2} \|X_2 - Y_2 + U_2\|_F \\
&= 2\frac{1}{2} \|D\mathbf{x} - \mathbf{s}\|_2^2 + 2\lambda \|\mathbf{y}\|_1 + \\
&\quad 2\frac{\rho}{2} \|\mathbf{x} - \mathbf{y} + \mathbf{u}\|_2 \\
&= 2L_\rho(X_1, Y_1, U_1) \tag{S4}
\end{aligned}$$

For this problem, the augmented Lagrangian for the $K = 2$ case is just twice the augmented Lagrangian for the $K = 1$ case, with the same penalty parameter ρ . Therefore we expect that the optimal penalty parameter should remain constant when changing the number of training images K .

B. Equality Constrained ADMM Dictionary Update

The augmented Lagrangian for the ADMM solution to the dictionary update problem Eq. (28) in the main document is

$$\begin{aligned}
L_\sigma(\mathbf{d}, \mathbf{g}, \mathbf{h}) &= \frac{1}{2} \|X\mathbf{d} - \mathbf{s}\|_2^2 + \iota_{C_{\text{PN}}}(\mathbf{g}) \\
&\quad + \frac{\sigma}{2} \|\mathbf{d} - \mathbf{g} + \mathbf{h}\|_2^2, \tag{S5}
\end{aligned}$$

where we omit the final term $-\frac{\sigma}{2} \|\mathbf{h}\|_2^2$, which does not effect the minimizer of this functional. For $K = 1$ we have $X_1 = X$, $\mathbf{s}_1 = \mathbf{s}$, $\mathbf{d}_1 = \mathbf{d}$, $\mathbf{g}_1 = \mathbf{g}$, and $\mathbf{h}_1 = \mathbf{h}$. If we construct the $K = 2$ case by replicating the training data, we have $X_2 = \begin{pmatrix} X & \\ & X \end{pmatrix}$, $\mathbf{s}_2 = \begin{pmatrix} \mathbf{s} \\ \mathbf{s} \end{pmatrix}$, $\mathbf{d}_2 = \mathbf{d}$, $\mathbf{g}_2 = \mathbf{g}$, and $\mathbf{h}_2 = \mathbf{h}$, and the augmented Lagrangian is

$$\begin{aligned}
L_\sigma(\mathbf{d}_2, \mathbf{g}_2, \mathbf{h}_2) &= \frac{1}{2} \|X_2\mathbf{d}_2 - \mathbf{s}_2\|_2^2 + \iota_{C_{\text{PN}}}(\mathbf{g}_2) \\
&\quad + \frac{\sigma}{2} \|\mathbf{d}_2 - \mathbf{g}_2 + \mathbf{h}_2\|_2^2 \\
&= 2\frac{1}{2} \|X\mathbf{d} - \mathbf{s}\|_2^2 + \iota_{C_{\text{PN}}}(\mathbf{g}) \\
&\quad + \frac{\sigma}{2} \|\mathbf{d} - \mathbf{g} + \mathbf{h}\|_2^2. \tag{S6}
\end{aligned}$$

For this problem, the augmented Lagrangian for the $K = 2$ case has a first term that is twice the augmented Lagrangian for the $K = 1$ case, while the second and third terms remain invariant with the same penalty parameter σ . Therefore we expect that the optimal penalty parameter should scale linearly when changing the number of training images K .

C. Consensus ADMM Dictionary Update

The augmented Lagrangian for the ADMM Consensus form of the dictionary update problem Eq. (39) in the main document is

$$\begin{aligned}
L_\sigma(\mathbf{d}, \mathbf{g}, \mathbf{h}) &= \frac{1}{2} \|X\mathbf{d} - \mathbf{s}\|_2^2 + \iota_{C_{\text{PN}}}(\mathbf{g}) \\
&\quad + \frac{\sigma}{2} \|\mathbf{d} - E\mathbf{g} + \mathbf{h}\|_2^2, \tag{S7}
\end{aligned}$$

where we omit the final term $-\frac{\sigma}{2} \|\mathbf{h}\|_2^2$, which does not effect the minimizer of this functional, and

$$E = \begin{pmatrix} I \\ I \\ \vdots \end{pmatrix}. \tag{S8}$$

For $K = 1$ we have $X_1 = X$, $\mathbf{s}_1 = \mathbf{s}$, $\mathbf{d}_1 = \mathbf{d}$, $\mathbf{g}_1 = \mathbf{g}$, and $\mathbf{h}_1 = \mathbf{h}$. If we construct the $K = 2$ case by replicating the training data, we have $X_2 = \begin{pmatrix} X & 0 \\ 0 & X \end{pmatrix}$, $\mathbf{s}_2 = \begin{pmatrix} \mathbf{s} \\ \mathbf{s} \end{pmatrix}$, $\mathbf{d}_2 = \begin{pmatrix} \mathbf{d} \\ \mathbf{d} \end{pmatrix}$, $\mathbf{g}_2 = \mathbf{g}$, and $\mathbf{h}_2 = \begin{pmatrix} \mathbf{h} \\ \mathbf{h} \end{pmatrix}$, and the augmented Lagrangian is

$$\begin{aligned}
L_\sigma(\mathbf{d}_2, \mathbf{g}_2, \mathbf{h}_2) &= \frac{1}{2} \|X_2\mathbf{d}_2 - \mathbf{s}_2\|_2^2 + \iota_{C_{\text{PN}}}(\mathbf{g}_2) \\
&\quad + \frac{\sigma}{2} \|\mathbf{d}_2 - E\mathbf{g}_2 + \mathbf{h}_2\|_2^2 \\
&= 2\frac{1}{2} \|X\mathbf{d} - \mathbf{s}\|_2^2 + \iota_{C_{\text{PN}}}(\mathbf{g}) \\
&\quad + 2\frac{\sigma}{2} \|\mathbf{d} - E\mathbf{g} + \mathbf{h}\|_2^2. \tag{S9}
\end{aligned}$$

For this problem, the first and third terms of the augmented Lagrangian for the $K = 2$ case are just twice the corresponding terms in the augmented Lagrangian for the $K = 1$ case, with the same penalty parameter σ , while the second term remains invariant. Therefore we expect that the optimal penalty parameter should remain constant when changing the number of training images K .

D. FISTA Dictionary Update

The FISTA solution to the dictionary update problem requires computing the gradient of the data fidelity term in the DFT domain (Eq. (59) in the main document)

$$\nabla_{\hat{\mathbf{d}}} \left(\frac{1}{2} \|\hat{X}\hat{\mathbf{d}} - \hat{\mathbf{s}}\|_2^2 \right) = \hat{X}^H (\hat{X}\hat{\mathbf{d}} - \hat{\mathbf{s}}). \tag{S10}$$

For $K = 1$ we have $\hat{X}_1 = \hat{X}$, $\hat{\mathbf{s}}_1 = \hat{\mathbf{s}}$ and $\hat{\mathbf{d}}_1 = \hat{\mathbf{d}}$. If we construct the $K = 2$ case by replicating the training data, we have $\hat{X}_2 = \begin{pmatrix} \hat{X} \\ \hat{X} \end{pmatrix}$, $\hat{\mathbf{s}}_2 = \begin{pmatrix} \hat{\mathbf{s}} \\ \hat{\mathbf{s}} \end{pmatrix}$, $\hat{\mathbf{d}}_2 = \hat{\mathbf{d}}$, and the gradient in the DFT domain is

$$\begin{aligned}
\nabla_{\hat{\mathbf{d}}_2} \left(\frac{1}{2} \|\hat{X}_2\hat{\mathbf{d}}_2 - \hat{\mathbf{s}}_2\|_2^2 \right) &= \hat{X}_2^H (\hat{X}_2\hat{\mathbf{d}}_2 - \hat{\mathbf{s}}_2) \\
&= 2\hat{X}^H (\hat{X}\hat{\mathbf{d}} - \hat{\mathbf{s}}). \tag{S11}
\end{aligned}$$

For this problem, the gradient in DFT domain for the $K = 2$ case is just twice the gradient in DFT domain for the $K = 1$ case. Therefore we expect that the optimal parameter L (i.e. the inverse of the gradient step size) should scale linearly when changing the number of training images K .

E. Mask Decoupling ADMM Sparse Coding

The augmented Lagrangian for the ADMM solution to the masked form of the MMV CBPDN problem Eq. (62) in the main document is

$$L_\rho(X, Y_0, Y_1, U_0, U_1) = \frac{1}{2} \|WY_1\|_F^2 + \lambda \|Y_0\|_1 + \frac{\rho}{2} \left\| \begin{pmatrix} Y_0 \\ Y_1 \end{pmatrix} - \left[\begin{pmatrix} I \\ D \end{pmatrix} X - \begin{pmatrix} 0 \\ S \end{pmatrix} \right] + \begin{pmatrix} U_0 \\ U_1 \end{pmatrix} \right\|_F^2, \quad (\text{S12})$$

where we omit the final term $-\frac{\rho}{2} \left\| \begin{pmatrix} U_0 \\ U_1 \end{pmatrix} \right\|_F^2$, which does not effect the minimizer of this functional. For $K = 1$ we have $S_1 = \mathbf{s}$, $X_1 = \mathbf{x}$, $Y_{01} = Y_0$, $Y_{11} = Y_1$, $U_{01} = U_0$ and $U_{11} = U_1$. If we construct the $K = 2$ case by replicating the training data, we have $S_2 = \begin{pmatrix} \mathbf{s} & \mathbf{s} \end{pmatrix}$, $X_2 = \begin{pmatrix} \mathbf{x} & \mathbf{x} \end{pmatrix}$, $Y_{02} = \begin{pmatrix} Y_0 & Y_0 \end{pmatrix}$, $Y_{12} = \begin{pmatrix} Y_1 & Y_1 \end{pmatrix}$, $U_{02} = \begin{pmatrix} U_0 & U_0 \end{pmatrix}$, $U_{12} = \begin{pmatrix} U_1 & U_1 \end{pmatrix}$, and $0_2 = \begin{pmatrix} 0 & 0 \end{pmatrix}$, and the augmented Lagrangian is

$$L_\rho(X_2, Y_{02}, Y_{12}, U_{02}, U_{12}) = \frac{1}{2} \|WY_{12}\|_F^2 + \lambda \|Y_{02}\|_1 + \frac{\rho}{2} \left\| \begin{pmatrix} Y_{02} \\ Y_{12} \end{pmatrix} - \begin{pmatrix} I \\ D \end{pmatrix} X_2 + \begin{pmatrix} 0_2 \\ S_2 \end{pmatrix} + \begin{pmatrix} U_{02} \\ U_{12} \end{pmatrix} \right\|_F^2 \\ = 2 \frac{1}{2} \|WY_{12}\|_F^2 + 2\lambda \|Y_{02}\|_1 + 2 \frac{\rho}{2} \left\| \begin{pmatrix} Y_0 \\ Y_1 \end{pmatrix} - \left[\begin{pmatrix} I \\ D \end{pmatrix} X - \begin{pmatrix} 0 \\ \mathbf{s} \end{pmatrix} \right] + \begin{pmatrix} U_0 \\ U_1 \end{pmatrix} \right\|_2^2 \\ = 2L_\rho(X, Y_0, Y_1, U_0, U_1) \quad (\text{S13})$$

For this problem, the augmented Lagrangian for the $K = 2$ case is just twice the augmented Lagrangian for the $K = 1$ case, with the same penalty parameter ρ . Therefore we expect that the optimal penalty parameter should remain constant when changing the number of training images K .

F. Mask Decoupling ADMM Dictionary Update

The augmented Lagrangian for the Block-Constraint ADMM solution of the masked dictionary update problem Eq. (71) in the main document is

$$L_\sigma(\mathbf{d}, \mathbf{g}_0, \mathbf{g}_1, \mathbf{h}_0, \mathbf{h}_1) = \frac{1}{2} \|W\mathbf{g}_1\|_2^2 + \iota_{\text{CPN}}(\mathbf{g}_0) + \frac{\sigma}{2} \left\| \begin{pmatrix} \mathbf{g}_0 \\ \mathbf{g}_1 \end{pmatrix} - \left[\begin{pmatrix} I \\ X \end{pmatrix} \mathbf{d} - \begin{pmatrix} 0 \\ \mathbf{s} \end{pmatrix} \right] + \begin{pmatrix} \mathbf{h}_0 \\ \mathbf{h}_1 \end{pmatrix} \right\|_2^2, \quad (\text{S14})$$

where we omit the final term $-\frac{\sigma}{2} \left\| \begin{pmatrix} \mathbf{h}_0 \\ \mathbf{h}_1 \end{pmatrix} \right\|_2^2$, which does not effect the minimizer of this functional. For $K = 1$ we have $X_1 = X$, $\mathbf{s}_1 = \mathbf{s}$, $\mathbf{d}_1 = \mathbf{d}$, $\mathbf{g}_{01} = \mathbf{g}_0$, $\mathbf{g}_{11} = \mathbf{g}_1$, $\mathbf{h}_{01} = \mathbf{h}_0$, and $\mathbf{h}_{11} = \mathbf{h}_1$. If we construct the $K = 2$ case by replicating the training data, we have $X_2 = \begin{pmatrix} X & X \end{pmatrix}$, $\mathbf{s}_2 = \begin{pmatrix} \mathbf{s} \\ \mathbf{s} \end{pmatrix}$, $\mathbf{d}_2 = \mathbf{d}$,

$\mathbf{g}_{02} = \mathbf{g}_0$, $\mathbf{g}_{12} = \begin{pmatrix} \mathbf{g}_1 \\ \mathbf{g}_1 \end{pmatrix}$, $\mathbf{h}_{02} = \mathbf{h}_0$, and $\mathbf{h}_{12} = \begin{pmatrix} \mathbf{h}_1 \\ \mathbf{h}_1 \end{pmatrix}$, and the augmented Lagrangian is

$$L_\sigma(\mathbf{d}, \mathbf{g}_{02}, \mathbf{g}_{12}, \mathbf{h}_{02}, \mathbf{h}_{12}) = \frac{1}{2} \|W\mathbf{g}_{12}\|_2^2 + \iota_{\text{CPN}}(\mathbf{g}_{02}) + \frac{\sigma}{2} \left\| \begin{pmatrix} \mathbf{g}_{02} \\ \mathbf{g}_{12} \end{pmatrix} - \begin{pmatrix} I \\ X_2 \end{pmatrix} \mathbf{d} + \begin{pmatrix} 0 \\ \mathbf{s}_2 \end{pmatrix} + \begin{pmatrix} \mathbf{h}_{02} \\ \mathbf{h}_{12} \end{pmatrix} \right\|_2^2, \\ = 2 \frac{1}{2} \|W\mathbf{g}_1\|_2^2 + \iota_{\text{CPN}}(\mathbf{g}_0) + \frac{\sigma}{2} \|\mathbf{g}_0 - \mathbf{d} + \mathbf{h}_0\|_2^2 + 2 \frac{\sigma}{2} \|\mathbf{g}_1 - (X\mathbf{d} - \mathbf{s}) + \mathbf{h}_1\|_2^2. \quad (\text{S15})$$

For this problem, the augmented Lagrangian for the $K = 2$ case has a first term that is twice the augmented Lagrangian for the $K = 1$ case, the second term remains invariant, while the third term (here split in two) has a mixed behavior. The top part of the third term remains invariant, but the bottom part is twice the bottom part of the $K = 1$ case. Therefore, there is no simple rule to scale the optimal penalty parameter σ when changing the number of training images K .

G. Hybrid Consensus Masked Dictionary Update

The augmented Lagrangian for the Consensus ADMM solution of the masked dictionary update problem Eq. (73) in the main document is

$$L_\sigma(\mathbf{d}, \mathbf{g}_0, \mathbf{g}_1, \mathbf{h}_0, \mathbf{h}_1) = \frac{1}{2} \|W\mathbf{g}_1\|_2^2 + \iota_{\text{CPN}}(\mathbf{g}_0) + \frac{\sigma}{2} \left\| \begin{pmatrix} I \\ X \end{pmatrix} \mathbf{d} - \begin{pmatrix} E & 0 \\ 0 & I \end{pmatrix} \begin{pmatrix} \mathbf{g}_0 \\ \mathbf{g}_1 \end{pmatrix} - \begin{pmatrix} 0 \\ \mathbf{s} \end{pmatrix} + \begin{pmatrix} \mathbf{h}_0 \\ \mathbf{h}_1 \end{pmatrix} \right\|_2^2, \quad (\text{S16})$$

where we omit the final term $-\frac{\sigma}{2} \left\| \begin{pmatrix} \mathbf{h}_0 \\ \mathbf{h}_1 \end{pmatrix} \right\|_2^2$, which does not effect the minimizer of this functional. For $K = 1$ we have $X_1 = X$, $\mathbf{s}_1 = \mathbf{s}$, $\mathbf{d}_1 = \mathbf{d}$, $\mathbf{g}_{01} = \mathbf{g}_0$, $\mathbf{g}_{11} = \mathbf{g}_1$, $\mathbf{h}_{01} = \mathbf{h}_0$, and $\mathbf{h}_{11} = \mathbf{h}_1$. If we construct the $K = 2$ case by replicating the training data, we have $X_2 = \begin{pmatrix} X & 0 \\ 0 & X \end{pmatrix}$, $\mathbf{s}_2 = \begin{pmatrix} \mathbf{s} \\ \mathbf{s} \end{pmatrix}$, $\mathbf{d}_2 = \begin{pmatrix} \mathbf{d} \\ \mathbf{d} \end{pmatrix}$, $\mathbf{g}_{02} = \mathbf{g}_0$, $\mathbf{g}_{12} = \begin{pmatrix} \mathbf{g}_1 \\ \mathbf{g}_1 \end{pmatrix}$, $\mathbf{h}_{02} = \begin{pmatrix} \mathbf{h}_0 \\ \mathbf{h}_0 \end{pmatrix}$, and $\mathbf{h}_{12} = \begin{pmatrix} \mathbf{h}_1 \\ \mathbf{h}_1 \end{pmatrix}$, and the augmented Lagrangian is

$$L_\sigma(\mathbf{d}, \mathbf{g}_{02}, \mathbf{g}_{12}, \mathbf{h}_{02}, \mathbf{h}_{12}) = \frac{1}{2} \|W\mathbf{g}_{12}\|_2^2 + \iota_{\text{CPN}}(\mathbf{g}_{02}) + \frac{\sigma}{2} \left\| \begin{pmatrix} I \\ X_2 \end{pmatrix} \mathbf{d}_2 - \begin{pmatrix} E & 0 \\ 0 & I \end{pmatrix} \begin{pmatrix} \mathbf{g}_{02} \\ \mathbf{g}_{12} \end{pmatrix} - \begin{pmatrix} 0 \\ \mathbf{s}_2 \end{pmatrix} + \begin{pmatrix} \mathbf{h}_{02} \\ \mathbf{h}_{12} \end{pmatrix} \right\|_2^2, \\ = 2 \frac{1}{2} \|W\mathbf{g}_1\|_2^2 + \iota_{\text{CPN}}(\mathbf{g}_0) + 2 \frac{\sigma}{2} \left\| \begin{pmatrix} I \\ X \end{pmatrix} \mathbf{d} - \begin{pmatrix} E & 0 \\ 0 & I \end{pmatrix} \begin{pmatrix} \mathbf{g}_0 \\ \mathbf{g}_1 \end{pmatrix} - \begin{pmatrix} 0 \\ \mathbf{s} \end{pmatrix} + \begin{pmatrix} \mathbf{h}_0 \\ \mathbf{h}_1 \end{pmatrix} \right\|_2^2. \quad (\text{S17})$$

For this problem, the first and third terms of the augmented Lagrangian for the $K = 2$ case are twice the corresponding terms in the augmented Lagrangian for the $K = 1$ case, with the same penalty parameter σ , while the second term remains invariant. Therefore we expect that the optimal penalty parameter should remain constant when changing the number of training images K .

SIV. EXPERIMENTAL SENSITIVITY ANALYSIS

Experiments to determine the stability of the optimal parameters across different training sets of the same size are discussed in Sec. VI-F2 in the main text. The corresponding results are plotted here in Figs. S4 – S15. The box plots represent median, quartiles, and spread of the normalized functional values obtained at each parameter value for the 20 different image subsets at each of the sizes $K \in \{5, 10, 20\}$. The red lines connect the medians of the distributions at each parameter value.

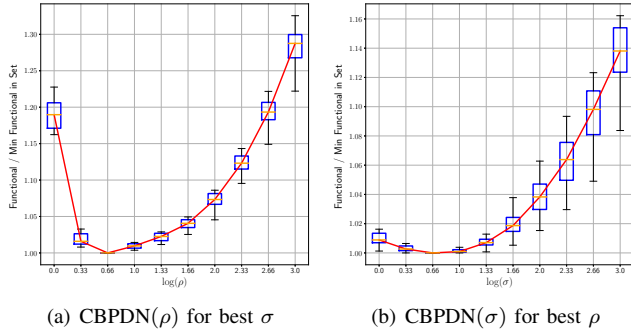


Fig. S4. Distribution of normalized CBPDN functional (Eq. (3) in the main document) after 100 iterations in conjugate gradient (CG) grid search for 20 random selected sets of $K = 5$ images.

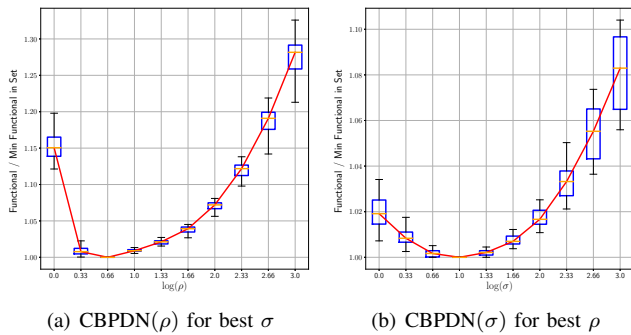


Fig. S5. Distribution of normalized CBPDN functional (Eq. (3) in the main document) after 100 iterations in conjugate gradient (CG) grid search for 20 random selected sets of $K = 10$ images.

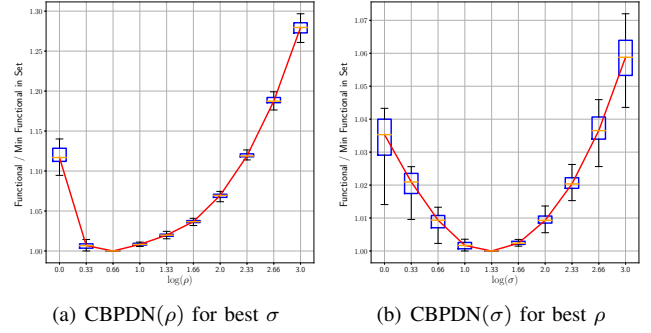


Fig. S6. Distribution of normalized CBPDN functional (Eq. (3) in the main document) after 100 iterations in conjugate gradient (CG) grid search for 20 random selected sets of $K = 20$ images.

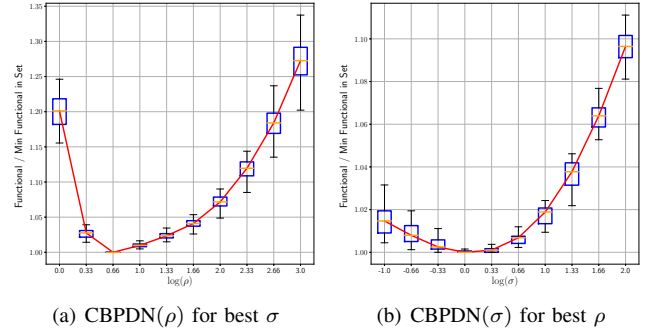


Fig. S7. Distribution of normalized CBPDN functional (Eq. (3) in the main document) after 100 iterations in consensus grid search for 20 random selected sets of $K = 5$ images.

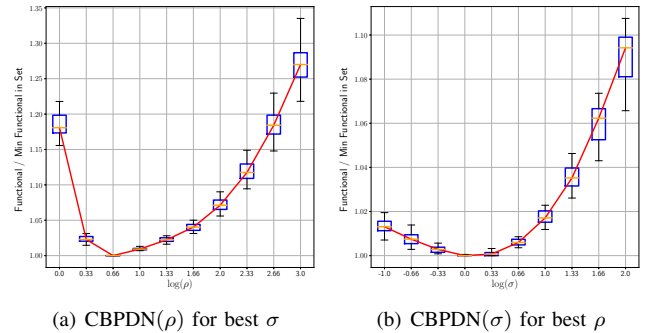


Fig. S8. Distribution of normalized CBPDN functional (Eq. (3) in the main document) after 100 iterations in consensus grid search for 20 random selected sets of $K = 10$ images.

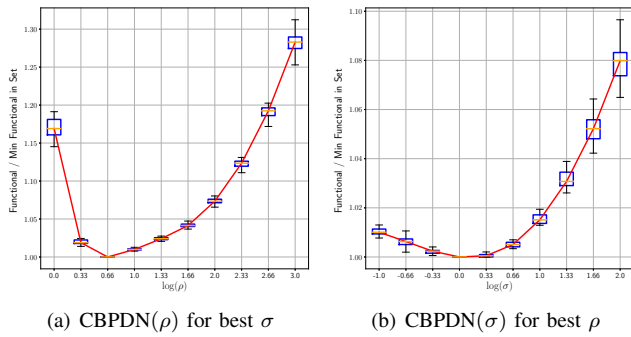


Fig. S9. Distribution of normalized CBPDN functional (Eq. (3) in the main document) after 100 iterations in consensus grid search for 20 random selected sets of $K = 20$ images.

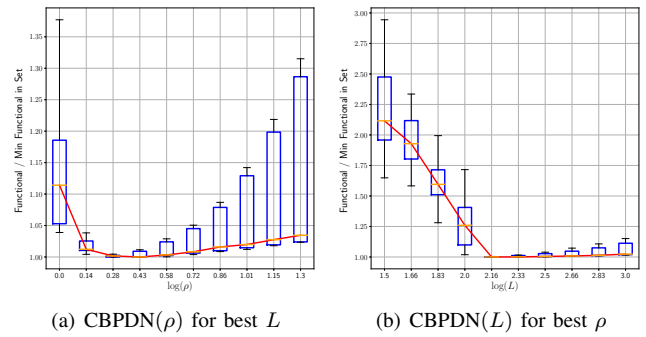


Fig. S12. Distribution of normalized CBPDN functional (Eq. (3) in the main document) after 100 iterations in FISTA grid search for 20 random selected sets of $K = 20$ images.

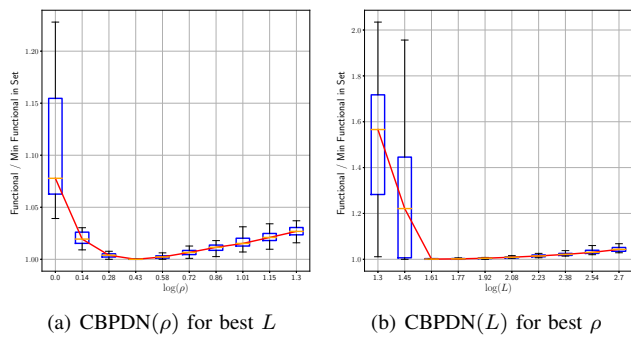


Fig. S10. Distribution of normalized CBPDN functional (Eq. (3) in the main document) after 100 iterations in FISTA grid search for 20 random selected sets of $K = 5$ images.

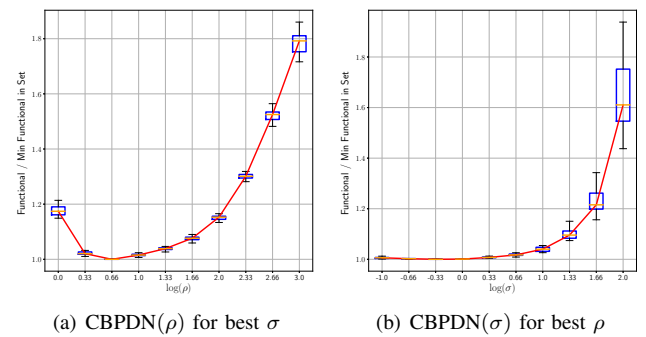


Fig. S13. Distribution of normalized masked CBPDN functional (Eq. (61) in the main document) after 100 iterations in masked consensus grid search for 20 random selected sets of $K = 5$ images.

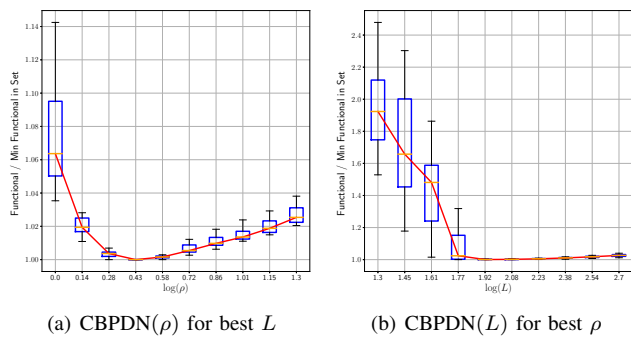


Fig. S11. Distribution of normalized CBPDN functional (Eq. (3) in the main document) after 100 iterations in FISTA grid search for 20 random selected sets of $K = 10$ images.

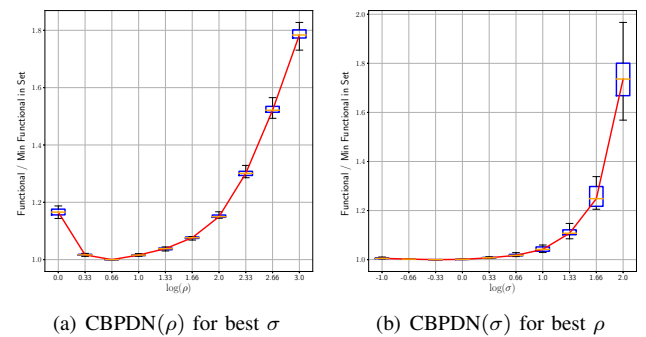


Fig. S14. Distribution of normalized masked CBPDN functional (Eq. (61) in the main document) after 100 iterations in masked consensus grid search for 20 random selected sets of $K = 10$ images.

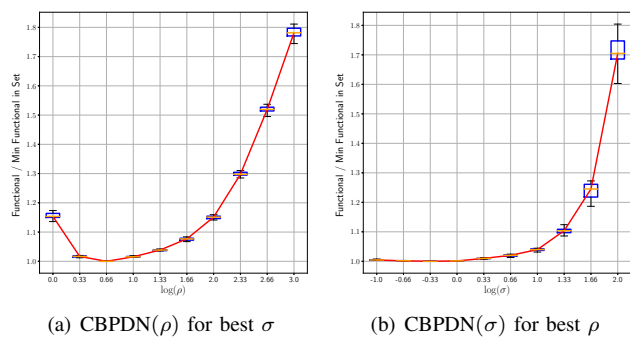


Fig. S15. Distribution of normalized masked CBPDN functional (Eq. (61) in the main document) after 100 iterations in masked consensus grid search for 20 random selected sets of $K = 20$ images.